Journal of Inflammation Research

Dovepress
Taylor & Francis Group

Open Access Full Text Article

ORIGINAL RESEARCH

Identification of Potential Diagnostic Biomarkers of Carotid Atherosclerosis in Obese Populations

Xize Wu[1,*], Jiaxiang Pan[2,*], Xue Pan[1,3,*], Jian Kang[1], Jiaqi Ren[1], Yuxi Huang[1], Lihong Gong[2,4], Yue Li[2,4]

[1]Graduate School, Liaoning University of Traditional Chinese Medicine, Shenyang, Liaoning, 110847, People's Republic of China; [2]Department of Cardiology, Affiliated Hospital of Liaoning University of Traditional Chinese Medicine, Shenyang, Liaoning, 110032, People's Republic of China; [3]College of Traditional Chinese Medicine, Dazhou Vocational College of Chinese Medicine, Dazhou, Sichuan, 635000, People's Republic of China; [4]Liaoning Provincial Key Laboratory of TCM Geriatric Cardio-Cerebrovascular Diseases, Shenyang, Liaoning, 110032, People's Republic of China

*These authors contributed equally to this work

Correspondence: Lihong Gong; Yue Li, Affiliated Hospital of Liaoning University of Traditional Chinese Medicine, No. 33, Beiling Street, Huanggu District, Shenyang, Liaoning, 110032, People's Republic of China, Tel +86 024-82961105, Email Linda1795@sina.com; med_liyue@163.com

Objective: This study aimed to investigate the potential mechanisms and biomarkers between Obesity (OB) and carotid atherosclerosis (CAS).

Methods: The GSE12828, GSE125771, GSE43292, and GSE100927 datasets were combined and normalized to obtain CAS-related differentially expressed genes (DEGs), and OB-related DEGs were obtained from the GSE151839 dataset and the GeneCards database. Unsupervised cluster analysis was conducted on CAS samples based on the DEGs of CAS and OB. Subsequently, immune infiltration analysis and gene set enrichment analysis (GESA) were performed. 61 machine learning models were developed to screen for Hub genes. The Single-gene GESA focused on calcium signaling pathway-related genes (CaRGs). Finally, high-fat diet-fed C57BL/6J ApoE$^{-/-}$ mice were used for in vivo validation.

Results: MMP9, PLA2G7, and SPP1 as regulators of the immune infiltration microenvironment in OB patients with CAS, and stratified CAS samples into subtypes with differences in metabolic pathways based on OB classification. Enrichment analysis indicated abnormalities in immune and inflammatory responses, the calcium signaling, and lipid response in obese CAS patients. The RF+GBM model identified CD52, CLEC5A, MMP9, and SPP1 as Hub genes. 15 CaRGs were up-regulated, and 12 were down-regulated in CAS and OB. PLCB2, PRKCB, and PLCG2 were identified as key genes in the calcium signaling pathway associated with immune cell infiltration. In vivo experiments showed that MMP9, PLA2G7, CD52, SPP1, FYB, and PLCB2 mRNA levels were up-regulated in adipose, aortic tissues and serum of OB and AS model mice, CLEC5A was up-regulated in aorta and serum, and PRKCB was up-regulated in adipose and serum.

Conclusion: MMP9, PLA2G7, CD52, CLEC5A, SPP1, and FYB may serve as potential diagnostic biomarkers for CAS in obese populations. PLCB2 and PRKCB are key genes in the calcium signaling pathway in OB and CAS. These findings offer new insights into clinical management and therapeutic strategies for CAS in obese individuals.

Keywords: carotid atherosclerosis, obesity, bioinformatics, unsupervised clustering analysis, machine learning model, calcium signaling pathway

Introduction

Obesity (OB) is characterized by excessive whole-body fat content and/or increased localized content and abnormal distribution.[1] The Report on Nutrition and Chronic Disease Status of Chinese Residents (2020) emphasized that the rate of OB among Chinese adults is 16.4% and the rate of overweight is 34.3%, which means that more than half of Chinese adults are overweight or obese.[2] This trend not only affects individual health but also imposes a heavy burden on the socio-economic system. The OB Society defines OB as a disease and the basis of many chronic diseases, increasing the

Received: 3 November 2024
Accepted: 29 January 2025
Published: 10 February 2025

likelihood of diseases such as diabetes, heart disease, sleep apnea, cancer, and other chronic diseases, as well as decreasing the life expectancy of patients.[3]

Atherosclerosis (AS) is a chronic inflammatory lesion occurring in the vascular wall characterized by lipid deposition and immune cell infiltration. AS primarily affects the medium and large arteries, including the carotid arteries, femoral arteries, and abdominal aorta, and underlies the pathology of many cardiovascular and cerebrovascular diseases.[4] A Mendelian randomization study has shown that OB increases the risk of cerebrovascular disease.[5] While carotid atherosclerosis (CAS) is more likely to cause ischemic cerebrovascular events. Therefore, the prevention of CAS in the obese population may reduce the risk of cardiovascular events.

OB is one of the well-known risk factors for AS, significantly increasing the incidence of atherosclerotic cardiovascular diseases. Although it is known that OB and AS share some pathophysiological mechanisms, such as abnormalities in lipid metabolism, insulin resistance, inflammation, endothelial dysfunction, adipokine imbalance, and inflammasome activation, the role of the calcium signaling pathway in OB and AS is not yet fully investigated.[6,7] The calcium signaling pathway plays a crucial role within cells; calcium ions are among the most common ions in the human body and act as a second messenger involved in a variety of physiological processes. Studies indicate that calcium signaling can alleviate OB by increasing metabolic rate and adipocyte differentiation, modulating neuronal excitability, enhancing energy expenditure, and curtailing food intake.[8] Furthermore, an elevated calcium intake has been correlated with a marked reduction in the risk of OB.[9,10] In the context of AS, the dysregulation of calcium signaling may affect AS by modulating inflammation, cell death, and the abnormal proliferation and migration of vascular smooth muscle cells (VSMCs), as well as through vascular calcification and promotion of plaque stability.[11,12] Such dysregulation may trigger abnormal behaviors of VSMCs, including uncontrolled proliferation, migration, and phenotypic transformation, which could promote the occurrence and progression of dyslipidemia and plaque.[13,14]

This study employed bioinformatics analysis to explore the potential mechanisms and biomarkers of CAS in obese populations, with a particular focus on calcium signaling pathway-related genes (CaRGs). Weighted Gene Co-expression Network Analysis (WGCNA) was utilized to discern molecular clusters and datasets, thereby identifying module genes, followed by the application of 61 machine learning models to screen for Hub genes. An in vivo comorbidity model was constructed to validate the expression of hub genes and CaRGs. Finally, a nomogram was developed to predict the risk of CAS in obstetric populations. The findings of this study underscore the significance of the calcium signaling pathway in the pathogenesis of OB and CAS and may offer new perspectives for future clinical practice and research.

Materials and Methods

Bioinformatics Analysis

Dataset Acquisition

The entire study process is depicted in Figures 1 and S1. The gene expression profiles of disease-related genes were searched by the Gene Expression Omnibus database (GEO, https://www.ncbi.nlm.nih.gov/geo/) under the keywords "atherosclerosis" and "obesity".[15] The CAS-related dataset GSE12828 includes mRNA sequencing data from 6 CAS samples;[16] the GSE125771 dataset includes mRNA sequencing data from 40 CAS samples;[17] the GSE43292 dataset includes mRNA sequencing data of arterial tissues from 32 CAS and 32 normal samples;[18] the GSE100927 dataset includes mRNA sequencing data of arterial tissues from 29 CAS and 12 normal samples;[19] the GSE28829 dataset includes mRNA sequencing data from 13 early CAS and 16 advanced samples;[20] and the OB-related dataset GSE151839 includes mRNA sequencing data of adipose tissue from 10 OB and 10 normal samples.[21] In addition, OB-related genes with a "relevance score" >5 were obtained from the GeneCards (http://www.genecards.org/) database. Among them, the GSE28829 dataset was used for external validation. The CaRGs were obtained from the MSigDB database under "c2.cp.kegg.symbols.gmt" (http://www.gsea-msigdb.org/gsea/msigdb/cards/KEGG_CALCIUM_SIGNALING_PATHWAY).

This study aims to include all relevant CAS datasets from the GEO database as much as possible; however, since there are fewer OB-related datasets in the GEO database, the GeneCards database is used to supplement OB-related genes.

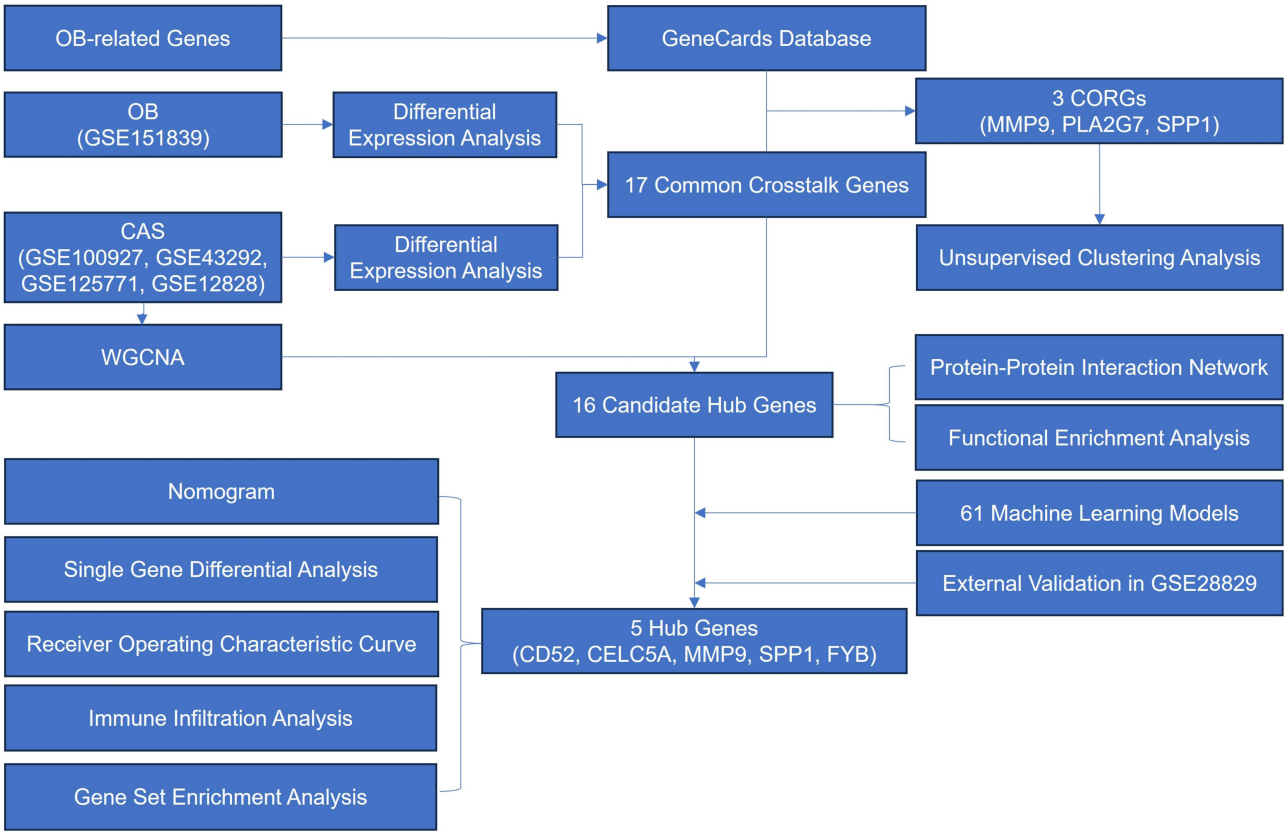

Figure 1 Flow chart of this study.

Identification of Differentially Expressed Genes (DEGs)

The CAS-related datasets GSE12828, GSE125771, GSE100927, and GSE43292 were merged and standardized using the "Affy" R package, while batch effects were removed with the "SVA" R package.[22,23] The "limma" R package was used to screen for DEGs that met $P<0.05$ and $|\log FC|>1$ (2-fold differential expression) between the disease and normal groups.[24] The DEGs of CAS and OB were intersected with OB-related genes to obtain CAS and OB co-related DEGs (CORGs).

Unsupervised Clustering Analysis of CAS Samples

Unsupervised clustering analysis of CAS samples based on CORGs expression profiles was performed using the "ConsensusClusterPlus" R package.[25] The CAS samples were grouped by applying the k-means algorithm with 1000 iterations, k=9, seed=123456, reps=50, pItem=0.8, pFeature=1, clusterAlg=km, distance=euclidean. The appropriate number of clusters was determined based on the matrix heat map, consistent cumulative distribution function curve, delta area plot, cluster-consensus plot, and item-consensus plot.

Immune Infiltration Analysis and Correlation Analysis

The degree of infiltration of 22 immune cells was quantified using the CIBERSORT deconvolution algorithm based on gene microarray data.[26] Differences between the two groups were compared using the Wilcox test. Subsequently, Spearman correlation analysis was employed to reveal the relationship between CORGs and immune cells.

Gene Set Variation Analysis (GSVA)

The "GSVA" package was used to conduct a GSVA enrichment analysis for different CORGs clusters, considering a significant change if the |t value of the GSVA score| was greater than 2.[27]

https://doi.org/10.2147/JIR.S504480

WGCNA

The "WGCNA" R package is used to remove the outlier samples and construct a co-expression network of gene expression matrices for the remaining samples. The soft threshold corresponding to fit R2=0.8 was chosen for the construction of gene modules, while the minimum number of module genes (minSize) was specified to be 10, and the most relevant module for the trait was selected.[28]

Functional Enrichment Analysis

Imported the genes into the David database (https://david.abcc.ncifcrf.gov/) and the Metascape database (https://metascape.org/gp/index.html) for functional enrichment and pathway analysis.[29–31] Similarly, genes were imported into the STRING database (https://cn.string-db.org/) to construct the protein-protein interaction (PPI) network.

Gene Set Enrichment Analysis (GSEA)

The "GSEA" R package is used to calculate the correlation between Hub genes and other genes, and then all genes are ranked according to the correlation from the highest to the lowest, and the enriched set of genes at the bottom of the ranking is detected and analyzed.[32]

Machine Learning Models Screening for Hub Genes

The "randomForestSRC" "glmnet" "plsRglm" "gbm" "caret" "mboost" "e1071" "BART" "MASS" "snowfall" "xgboost" R packages were used to establish 61 machine learning models screening for the hub genes, including the least absolute shrinkage and selection operator (LASSO) regression, random forest (RF) model, support vector machine model (SVM), support vector machine-recursive feature elimination (SVM-RFE), generalized linear model (GLM), gradient boosting machine (GBM), and extreme gradient boosting (XGBoost), gradient boosting machine, and so on.[33] The merged dataset of GSE100927, GSE43292, GSE12828, and GSE125771 was used as a training set, and the GSE28829 dataset was used as a validation set. The area under the receiver operating characteristic (ROC) curve was visualized using the "pROC" R package.[34] F1 scores were calculated based on precision and recall; weighted scores were calculated based on F1 scores, area under the curve (AUC) values, and accuracy, and then the best models were screened based on the AUC values, accuracy, F1 scores, gene counts, and weighted scores. The optimal machine learning model was identified and externally validated using the Wilcoxon rank-sum test for single gene difference analysis on the GSE28829 dataset.

Construction and Validation of a Nomogram Model

A nomogram model was established using the "rms" R package to predict the probability of the occurrence of AS, and its predictive power was estimated by using calibration curves and decision curve analysis. The AUC of the ROC was then calculated for each key gene to test the diagnostic efficacy of the Hub genes.

Construction of "miRNA-mRNA" Networks

CORGs and Hub genes were imported into the TargetScan (http://www.targetscan.org/vert_72/), TarBase (https://dianalab.e-ce.uth.gr/tarbasev9), miRmap (https://mirmap.ezlab.org/), and miRDB databases (https://mirdb.org/) to predict miRNAs and required to be predicted by at least three databases to construct "miRNA-mRNA" networks.

Statistical Analysis

All Statistical Analyses Were Performed Using R Software, and $P<0.05$ Was Considered Significant

In Vivo Experimental Validation

Experimental Animal

10 SPF-grade male C57BL/6J mice were fed a normal diet as the control group, and 10 male C57BL/6J ApoE$^{-/-}$ mice were fed a high-fat diet (XIAOSHUYOUTAISHIYANDONGWUSILIAO, Cat.D12109C) for 12 weeks as the model group. The experimental animals were purchased from the Liaoning Changsheng Biotechnology Co., Ltd., aged 6–-8 weeks, weighting 18–22 g, the animals were housed and experimented with in the Experimental Animal Center of the Affiliated Hospital of Liaoning University of TCM. Feeding conditions: 12 h alternating light and dark, room temperature (22±1) °C, relative humidity 45%-55%, normal chow diet, free dietary water, and the experiments were started after

Table 1 A List of the Primers Used in the qRT-PCR

Gene	Primer sequence (5'-3')
GAPDH	Forward: CCTCGTCCCGTAGACAAAATG
	Reverse: TGAGGTCAATGAAGGGGTCGT
MMP9	Forward: CTGGACAGCCAGACACTAAAG
	Reverse: CTCGCGGCAAGTCTTCAGAG
CLEC5A	Forward: ATGCCTACAAGGAGCTATGGAAC
	Reverse: CAAGGTGATTCGGAGAAGGAGA
CD52	Forward: CAAAAACAGCACCTCCACCAA
	Reverse: TTGGGATGTCTCTCGCTACTGAT
PLA2G7	Forward: AGCGTCTTCGTGCGTTTGTA
	Reverse: GCCAATAGCAGAATAAATCGTCC
SPP1	Forward: AGCAAGAAACTCTTCCAAGCAA
	Reverse: GTGAGATTCGTCAGATTCATCCG
FYB	Forward: TCAACACGGGGAGTAACCC
	Reverse: CGAGCTTTGTCCTGCAACT
PLCB2	Forward: CAACCACTTCCTGCTGAAAACACT
	Reverse: CCAGTCCTTGCCTACGTTCTCC
PLCG2	Forward: GTGGACACCCTTCCAGAATATG
	Reverse: ACCTGCCGAGTCTCCATGAT
PRKCB	Forward: AGCGAGACACCTCCAACTTC
	Reverse: CAGTGGGAGTCAGTTCCACAG

7 days of acclimatization feeding. Assess the success of the mouse OB model by evaluating changes in body weight and Lee's index. Evaluate the success of the mouse AS model through histological examination of the aorta using hematoxylin-eosin (HE) and oil red O (ORO) staining. Lee's index = [body weight (g)^(1/3)]/body length (cm).

Oil Red O (ORO) Staining

The aorta was subjected to frozen sections, stained with ORO dye (Servicebio, Cat.G1015) for 10 min, and then removed, differentiated in 70% ethanol, washed in distilled water, observed under the microscope, and photographed.

HE Staining

The aorta was subjected to paraffin sectioning, gradually dewaxed, dipped in hematoxylin (Servicebio, Cat.G1002) for 8–15 min, washed to remove hematoxylin and floating color for 1–2 min, differentiated, washed in running pure water for 30–60 min, dipped in eosin solution (Servicebio, Cat.G1004) for 2–5 min, dehydrated, transparent, sealed, and baked, and photographed for observation under the microscope (Nikon, Eclipse Ci).

Quantitative Real-Time Polymerase Chain Reaction (qRT-PCR)

Total RNA was extracted from cell lines using a Trizol total RNA isolation reagent and treated with Turbo DNase. cDNA was synthesized from total RNA (0.5 mg) using random hexamers with the TaqMan cDNA Reverse Transcription Kit. Primers were designed using Primer Express v3.0 software, and real-time PCR was performed using SYBR Select Master Mix (Applied Bio-Systems). All reactions were carried out on the 7500 Fast Real-Time PCR System. The average of six independent analyses for each gene and sample was calculated using the DD threshold cycle (Ct) method and normalized to the endogenous reference control gene. The above primers were synthesized by Sangon Biotech (Shanghai) Co., Ltd. (https://www.sangon.com/) (Table 1).

Results

Identification of CAS-Related Genes in the OB Population

Identification of DEGs for AS and OB

The CAS-related datasets GSE12828, GSE125771, GSE100927, and GSE43292 were first merged and normalized. Prior to merging, the datasets exhibited some differences, but after merging and removing batch effects, the data showed a certain degree of similarity (Figure 2A and B). Differential expression analysis identified 79 DEGs for CAS and 254

DEGs for OB (P<0.05 and |logFC|>1), with 17 DEGs showing concordant expression (Figure 2C). Then 563 OB-related genes (relevance score >5) were obtained from the GeneCards database, and three CORGs (MMP9, PLA2G7, and SPP1) were obtained by intersecting with the above genes, which were up-regulated in OB and AS patients (Figure 2D and E). Correlation analysis showed significant coordination between MMP9 and PLA2G7, and SPP1 (Figure 2F). To determine the potential functions of these genes in CAS, the GSEA results indicated that the pathogenesis of CAS mainly involves various cardiomyopathies, tyrosine metabolism, lysosomal, apoptosis, the JAK-STAT, PPAR, TOLL-like receptor, and calcium signaling pathways (Figure 2G and H).

To further understand the immune microenvironment of CAS, the results of immune infiltration analysis showed that memory B cells, follicular helper T cells, γ-δ T cells, and M0 macrophages had a higher abundance in CAS, while naïve B cells, plasma cells, CD8 T cells, resting memory CD4 T cells, activated NK cells, monocytes, M2 macrophages, and resting mast cells had a lower abundance in CAS (P<0.05) (Figure 2I). Furthermore, correlation analysis showed that CORGs were significantly negatively correlated with naïve B cells, monocytes, plasma cells, resting memory CD4 T cells, and CD8 T cells, and significantly positively correlated with M0 macrophages, suggesting that CORGs regulate the immune infiltration microenvironment of CAS (P<0.05) (Figure 2J).

Identification of Molecular Clusters of OB Subtypes in CAS Samples

Initially, the consensus cumulative distribution function and the delta area inflection method were employed to determine the most suitable value of k. These methods suggested that k values of 2, 3, or 4 are preferable (Figure 3A and B). Further examination through the matrix heatmap revealed that when the CAS were partitioned into 2 or 3 clusters, the resulting groups were well-defined with minimal overlap, indicating a clear separation. Conversely, when the data was segmented into 4 clusters, the C3 and C4 clusters exhibited increased clutter, with higher levels of intermingling and similarity, leading to a less stable clustering pattern (Figure 3C). Consequently, the option of k=4 was deemed unsuitable Subsequent analysis using the item-consensus plot and cluster-consensus plot corroborated the initial findings, with k=2 or k=3 yielding clusters that were more distinct and stable (Figure 3D–F). A detailed differential analysis was then performed for k=3, which categorized the 107 CAS samples into three distinct clusters: the C1 cluster (n=48), the C2 cluster (n=18), and the C3 cluster (n=41). Within these clusters, genes MMP9, PLA2G7, and SPP1 were found to be highly expressed, particularly in clusters C1 and C3. When k was reduced to 2, the CAS samples were consolidated into two clusters: the C1 cluster (n=83) and the C2 cluster (n=24). In this configuration, the genes MMP9, PLA2G7, and SPP1 were again observed to be highly expressed, predominantly in the C1 cluster (Figure 3G). Upon reviewing the classification of individual samples, it was noted that the C1 and C3 clusters identified at k=3 were subsumed within the C1 cluster at k=2. This observation, coupled with the fact that the C1 and C3 clusters at k=3 were not significantly distinct and exhibited lower stability, led to the conclusion that a k value of 2 provided a more robust and coherent clustering solution. Therefore, k=2 was selected as the optimal number of clusters for this dataset.

Further immune infiltration analysis revealed a higher prevalence of follicular helper T cells, regulatory T cells, γ-δ T cells, M0 macrophages, and activated mast cells in the C1 cluster, whereas the C2 cluster had a higher abundance of naïve B cells, plasma cells, CD8 T cells, resting memory CD4 T cells, activated NK cells, monocytes, M1 macrophages, M2 macrophages, activated dendritic cells, and resting mast cells (Figure 3H).

GSVA indicated that the C2 cluster was mainly involved in processes such as retinol metabolism, inositol phosphate metabolism, linolenic acid metabolism, the calcium signaling pathway, and the hedgehog signaling pathway. On the other hand, the C1 cluster was primarily associated with porphyrin and chlorophyll metabolism, glycerophospholipid metabolism, sulfur metabolism, glutathione metabolism, the B-cell receptor signaling pathway, and the Fc gamma R-mediated phagocytosis. These findings suggest that, according to OB typing, CAS samples can be divided into two subgroups with significantly different metabolic types (Figure 3I).

Identification and Functional Enrichment Analysis of Candidate Hub Genes

The WGCNA was performed across all samples to identify the co-expression modules that are most relevant to CAS (Figure 4A). Upon setting the soft threshold to 15 (Figure 4B), three distinct modules were delineated, among which the "turquoise" module exhibited a significant positive correlation with CAS (r=0.65) and contained 1221 module genes

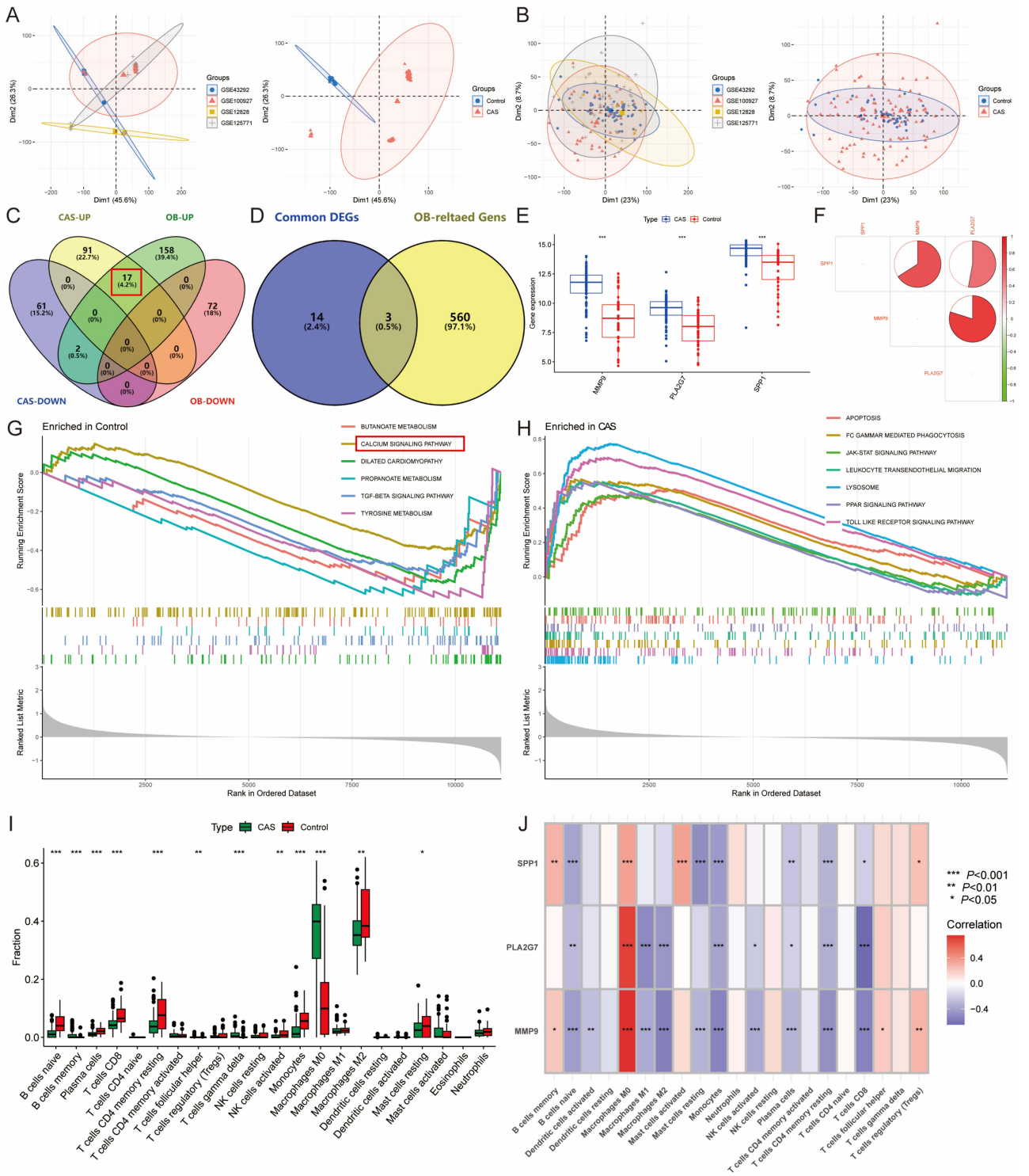

Figure 2 Identification of CAS differentially expressed genes (DEGs) by differential expression analysis. (**A**). The principal component analysis (PCA) of the four datasets and clinical characteristics. (**B**). The PCA of the combined dataset and clinical characteristics. (**C**). Venn diagram showing 17 common DEGs of CAS and OB. (**D**). Venn diagram showing 3 CAS and OB co-related DEGs (CORGs). (**E**). Boxplot showing the differential expression of CORGs in CAS. (**F**). Correlation analysis between CORGs. (**G** and **H**). The GSEA for CAS (**G**) and control (**H**) samples. (**I**). Boxplot showing differences in immune infiltration between CAS and control groups. (**J**). Correlation analysis of the CORGs with infiltrating immune cells. **P*<0.05, ***P*<0.01, ****P*<0.001.

https://doi.org/10.2147/JIR.S504480

https://doi.org/10.2147/JIR.S504480

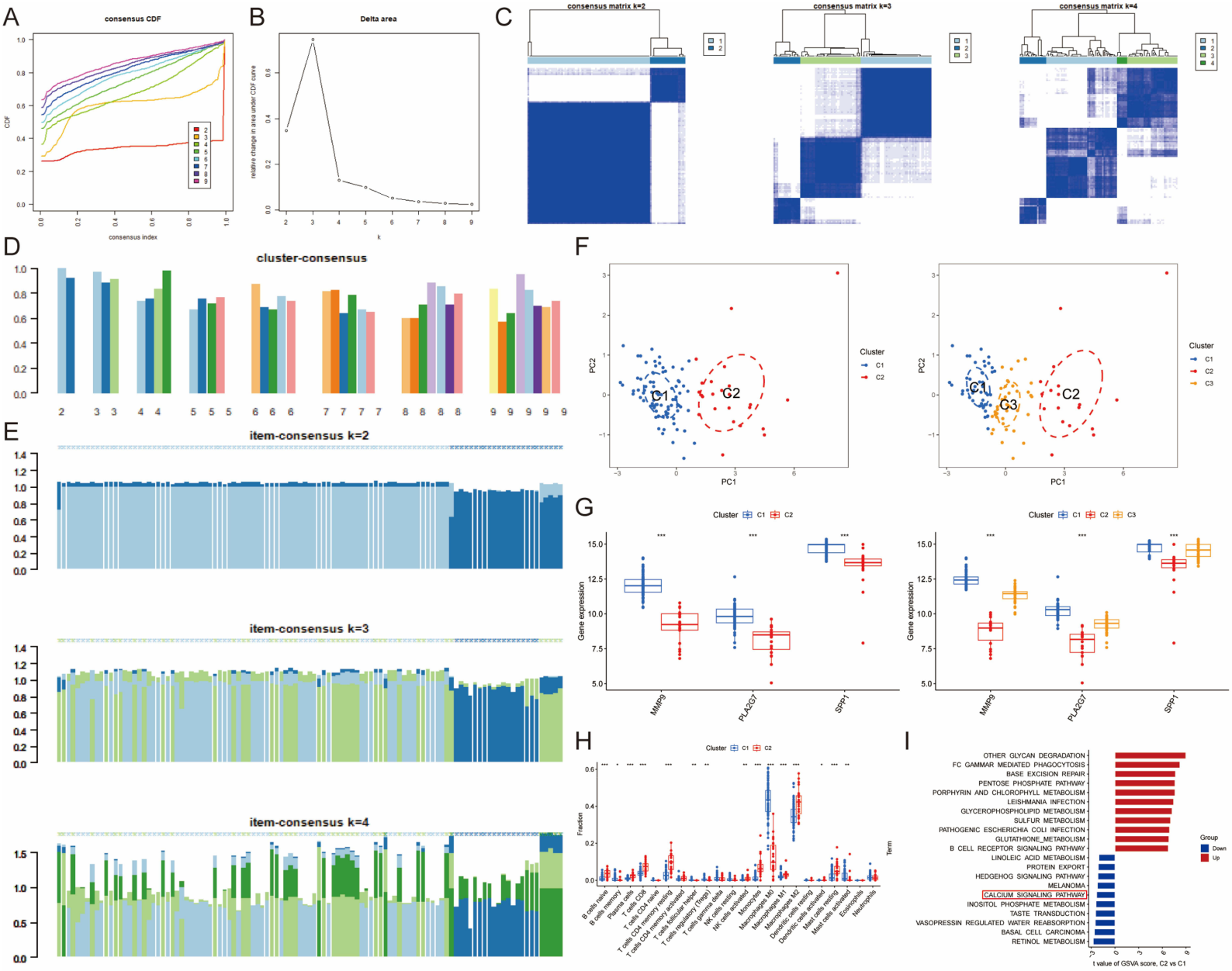

Figure 3 Identification of obesity-related molecular clusters in CAS patients. (**A-B**). Representative (**A**) cumulative distribution function (CDF) curves and (**B**) delta area curves. (**C**). Consensus clustering matrix when k=2, 3, and 4. (**D**). cluster-consensus plot. (**E**). The item-consensus plot when k=2, 3, and 4. (**F**). The PCA showing subtype distribution when k=2 and 3. (**G**). The boxplot of expression levels of the 3 CORGs between the two and three obesity molecular clusters. (**H**). Comparison of immune cell infiltration between two clusters. (**I**). The GSVA analysis of C1 and C2 clusters. **P*<0.05, ***P*<0.01, ****P*<0.001.

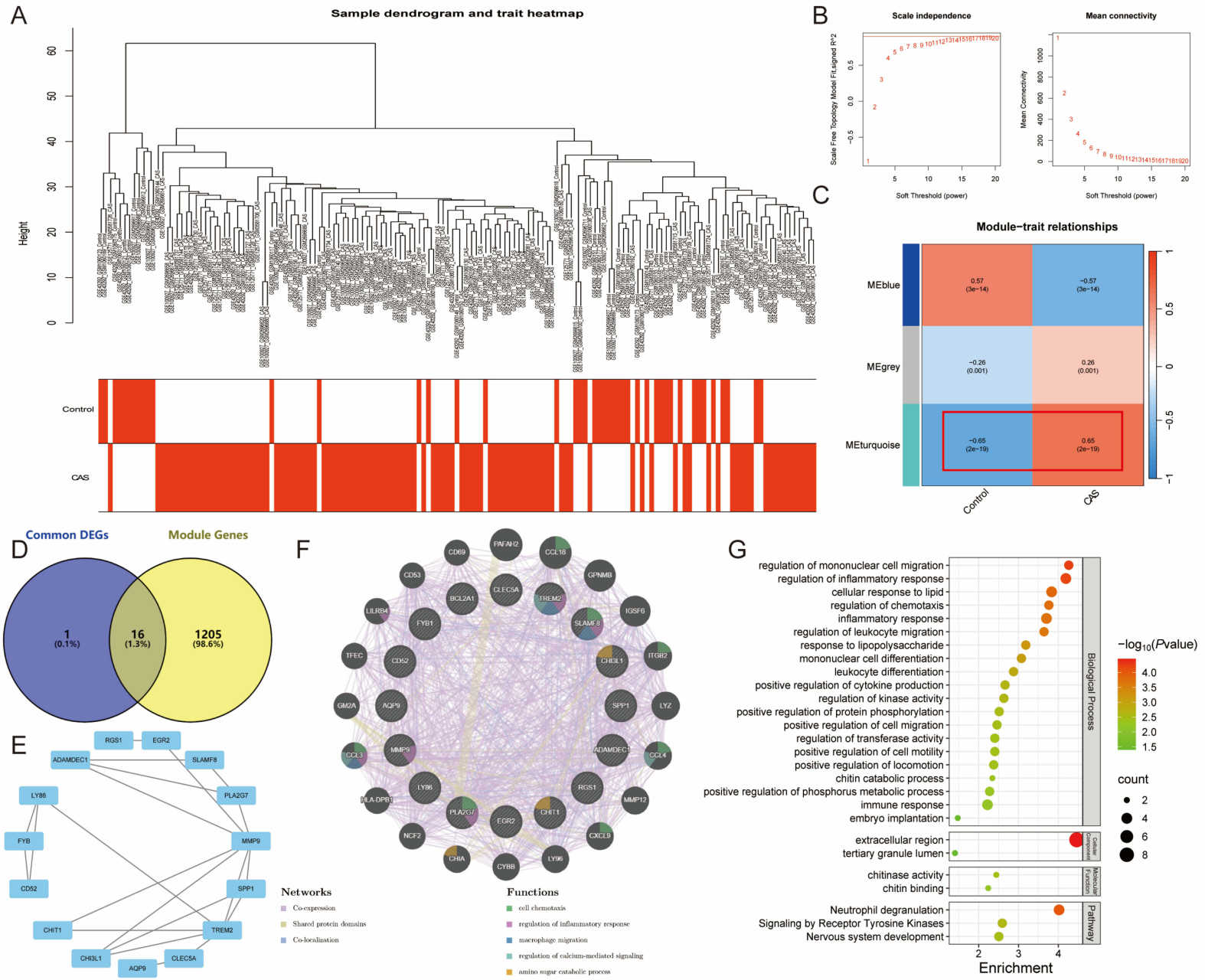

Figure 4 Identification and enrichment analysis of candidate Hub genes. (**A**). The sample clustering plot of all samples after removing outlier samples. (**B**). Soft threshold selection 15. (**C**). Module genes related to CAS traits. (**D**). Venn diagram showing 16 candidate Hub genes. (**E** and **F**). PPI network of candidate Hub genes. (**G**). The pathway, biological process, cellular component, and molecular function enrichment analysis of candidate Hub genes.

https://doi.org/10.2147/JIR.S504480

(Figure 4C). The module genes and DEGs of CAS and OB were intersected to obtain 16 candidate Hub genes (Figure 4D and E), which upon functional enrichment analysis revealed that the pathogenesis of OB and CAS is related to biological processes such as immune response, inflammatory response, inflammatory cell migration (regulation of mononuclear cell migration and leukocyte migration, positive regulation of cell migration and cell motility), cellular response to lipid, cellular differentiation (mononuclear cell and leukocyte differentiation), chitinase activity, chitin binding, neutrophil degranulation, signaling by receptor tyrosine kinases, the calcium signaling pathway, and nervous system development (Figure 4F and G). This suggests that the pathogenesis of CAS in the obese population involves abnormalities in several biological processes, including the immune response, inflammatory response, cellular chemotaxis, the calcium signaling pathway, and cellular response to lipids.

Identification and Validation of Hub Genes

To enhance the detection of potential biomarkers for CAS in the obese population, 61 machine learning models were developed to identify Hub genes and mitigate the risk of overfitting. The GBM, Stepglm [forward], RF+GBM, and RF models demonstrated strong diagnostic capabilities, as evidenced by their mean AUC values, accuracy, F1 scores, and weighted scores from both the training set and the GSE28829 validation set. However, the GBM and Stepglm [forward] models, particularly when utilizing 16 genes, exhibited a propensity for overfitting and were therefore excluded from further consideration. Moreover, the RF+GBM model outperformed the RF model in terms of individual and average AUC, accuracy, and F1 score, leading to its selection as the optimal model (Figure 5A). The model encompassed 6 genes: EGR2, CD52, SPP1, FYB, MMP9, and CLEC5A. Subsequent external validation through single-gene differential expression analysis confirmed the differential expression of CD52, CLEC5A, FYB, MMP9, and SPP1, while EGR2 did not show significant differential expression (Figure 5B).

To further validate the expression of the Hub gene, a co-morbidity model of OB and AS was constructed using high-fat diet-fed C57BL/6J ApoE$^{-/-}$ mice, and adipose, aortic tissues and serum were taken for experimental validation. In vivo experiments demonstrated that mice fed a high-fat diet exhibited a significant increase in body weight, averaging 35.634±0.690 g (n=10), compared to the control group mice with an average weight of 26.367±0.451 g (n=10). The Lee's index of the model group was significantly elevated at 0.396±0.009 (n=10) compared to the control group at 0.323±0.013 (n=10). Histological examination of the aortas from the model group, as revealed by HE and ORO staining, indicated intimal hyperplasia, irregular cellular arrangement, and vacuolation, along with lipid deposition (Figure 6A). These findings confirm the successful establishment of the OB and AS mouse models. The mRNA gene expression levels of MMP9, PLA2G7, SPP1, FYB and CD52 were significantly higher in the aorta and adipose tissue and serum of the model mice compared to the control group; whereas CLEC5A was up-regulated in the aorta and serum (Figure 6B). Thus, PLA2G7, CD52, CLEC5A, FYB, MMP9, and SPP1 were identified as Hub genes.

Construction and Validation of Nomogram

Subsequently, this study developed a Hub gene-based nomogram to predict the risk of CAS in obese population (Figure 7A). Decision and calibration curves demonstrated that the predictive model, based on these hub genes, exhibited excellent diagnostic efficacy and was effective in assessing the risk of CAS among the obese population (Figure 7B and C). The ROC curves for the internal training set and the external validation set (GSE28829) demonstrated that the Hub genes possessed robust diagnostic efficacy, with an AUC exceeding 0.75 (Figure 7D and E).

To gain a deeper understanding of the molecular links between OB and CAS, and to identify potential biomarkers and therapeutic targets, subsequent predictions of miRNAs associated with Hub genes were made using databases. These miRNAs may play a crucial regulatory role in the pathological processes of OB and CAS. Specifically, the miRNAs corresponding to CLEC5A as hsa-miR-130b-5p and hsa-miR-4753-3p, CD52 to hsa-miR-214-5p, MMP9 to hsa-miR -3065-5p, PLA2G7 to hsa-miR-214-5p, SPP1 to hsa -miR-130b-5p, hsa-miR-4753-3p, and hsa-miR-3065-5p (Figure 7F).

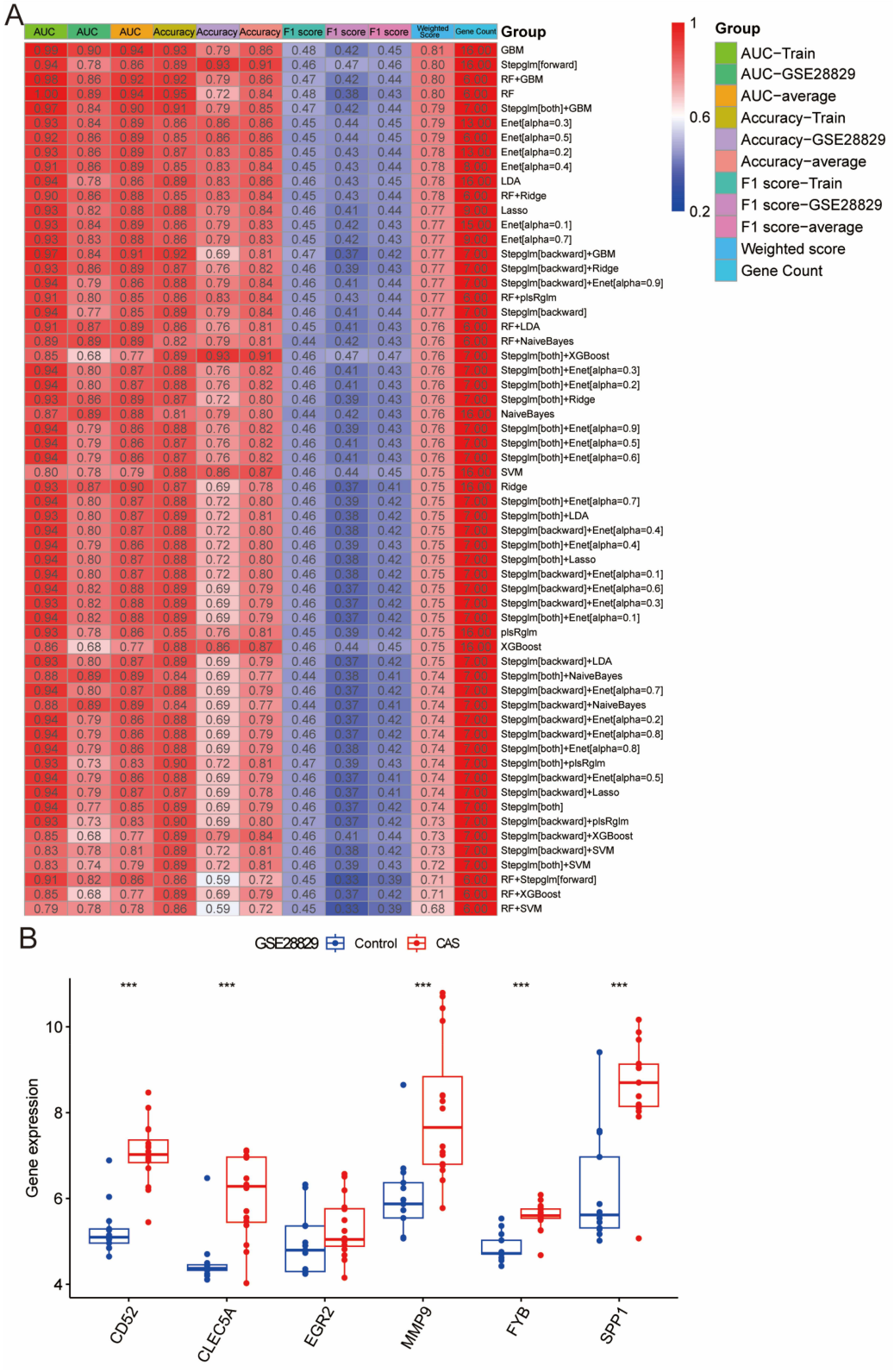

Figure 5 Construction and assessment of machine learning models. (**A**). Construction of 61 machine learning models to screen for hub genes. The best models were screened based on AUC values, accuracy, F1 scores, and gene counts. (**B**). Single-gene differential analysis was performed in the validation set GSE28829 to screen for Hub genes. ***P<0.001.

https://doi.org/10.2147/JIR.S504480

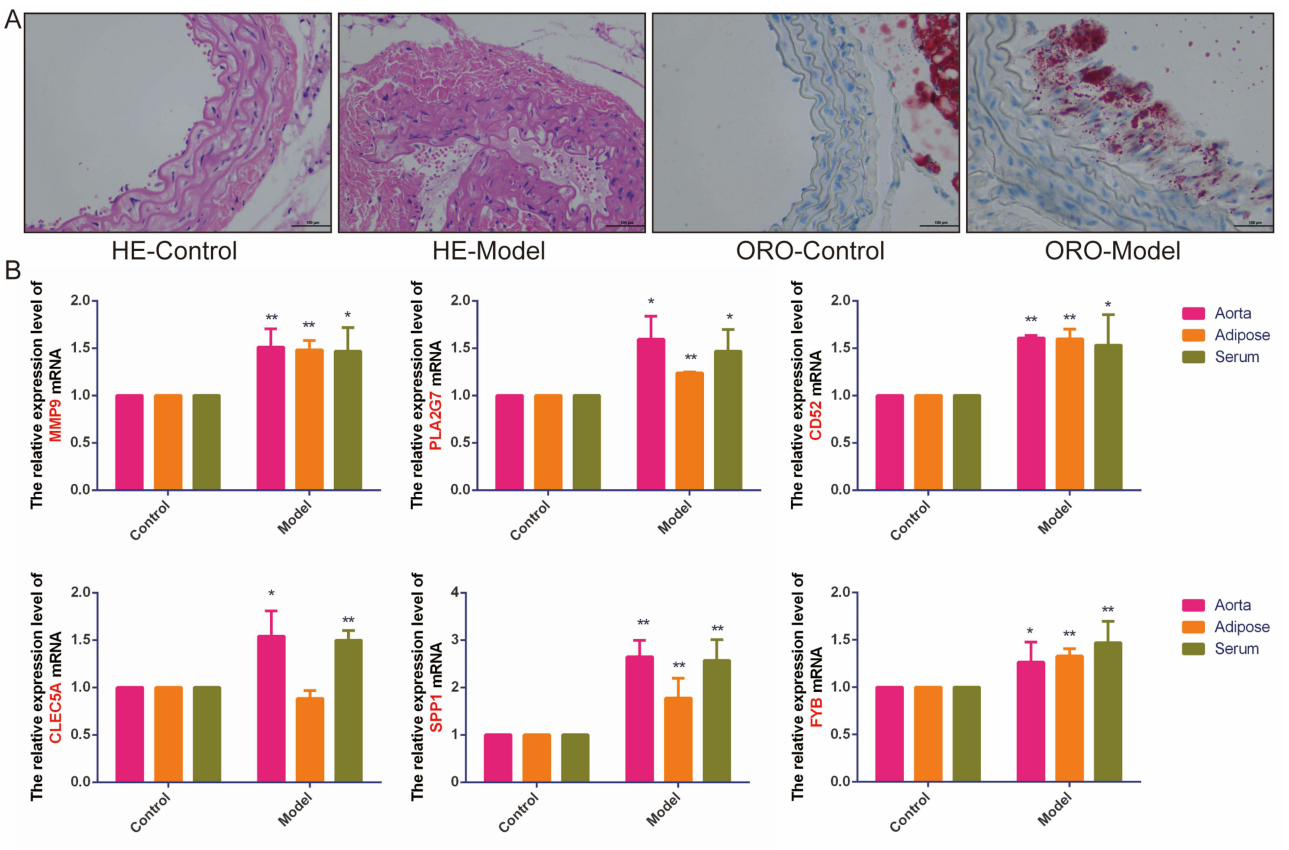

Figure 6 In vivo experiments to verify Hub gene expression. (**A**). HE and ORO pathological staining of aorta (n=6, bar=100μm). (**B**). The relative expression level of MMP9, PLA2G7, CD52, CLEC5A, SPP1, and FYB genes (n=6). *P<0.05 vs the Control group, **P<0.01 vs the Control group.

Identification of Key Genes and Subtypes of the Calcium Signaling Pathway in OB and CAS

Identification of Calcium Signaling Pathway-Related Genes in the OB and CAS

The previous results of GSEA (P=0.0014) indicated that substantial enrichment of the calcium signaling pathway was significantly enriched in CAS (Figure 8A). To elucidate the role of this pathway in the development of OB and CAS, "GSVA" was utilized to identify 178 CaRGs, of which 27 genes were significantly different between the two groups (P<0.05), 15 CaRGs were up-regulated, while 12 CaRGs were down-regulated in CAS and OB, suggesting that the calcium signaling pathway could be a pivotal pathway in the pathogenesis of both OB and CAS.

Enrichment analyses have revealed that the biological functions of the 27 identified CaRGs are multifaceted. In addition to their established role in calcium transport, these genes are also implicated in the adenylate cyclase-activating G protein-coupled receptor signaling pathway, positive regulation of angiogenesis, inflammatory response, positive regulation of interleukin-6 production, phosphatidylinositol metabolic process, and lipid catabolic process. These genes are predominantly associated with components involved in calcium transport, with a particular focus on the plasma membrane, membrane rafts, presynaptic terminals, glutamatergic synapses, the phosphorylase kinase complex, Schaffer collateral-CA1 synapses, neuronal cell bodies, and the cAMP-dependent protein kinase complex. Molecular function with calmodulin binding, phospholipase C activity, phosphatidylinositol phospholipase C activity, ATP binding, phosphorylase kinase activity, prostaglandin E receptor activity, cAMP-dependent protein kinase activity, glutamate receptor binding, and adenylate cyclase activity. These genes are also associated with the regulation of the phospholipase D signaling pathway, VSMCs contraction, aldosterone synthesis and secretion, inflammatory mediator regulation of TRP channels, regulation of TRP channels, cGMP-PKG signaling pathway, chemokine signaling pathway, platelet activation, and regulation of lipolysis in adipocytes.

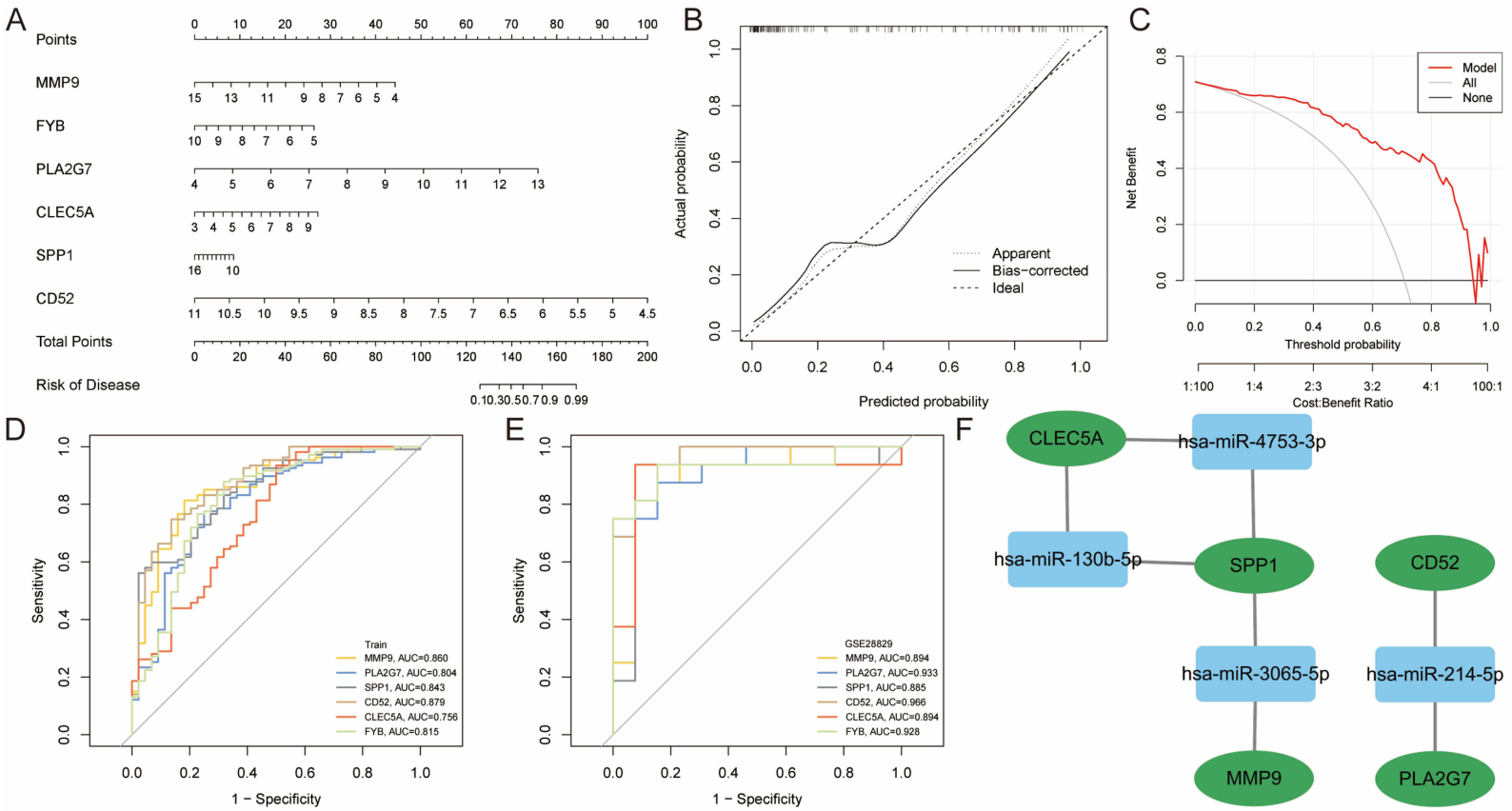

Figure 7 Construction and validation of nomogram to predict the risk of developing CAS in obese population. (**A**). Construction of a nomogram based on the Hub gene's RF+GBM model. (**B** and **C**). Construction of a (**B**) calibration curve and (**C**) decision curve analysis for assessing the predictive efficiency of the nomogram model. (**D** and **E**). The (**D**) internal and (**E**) external validation of ROC curves for diagnostic efficacy of Hub genes. (**F**). "miRNA-mRNA (Hub genes)" network.

https://doi.org/10.2147/JIR.S504480

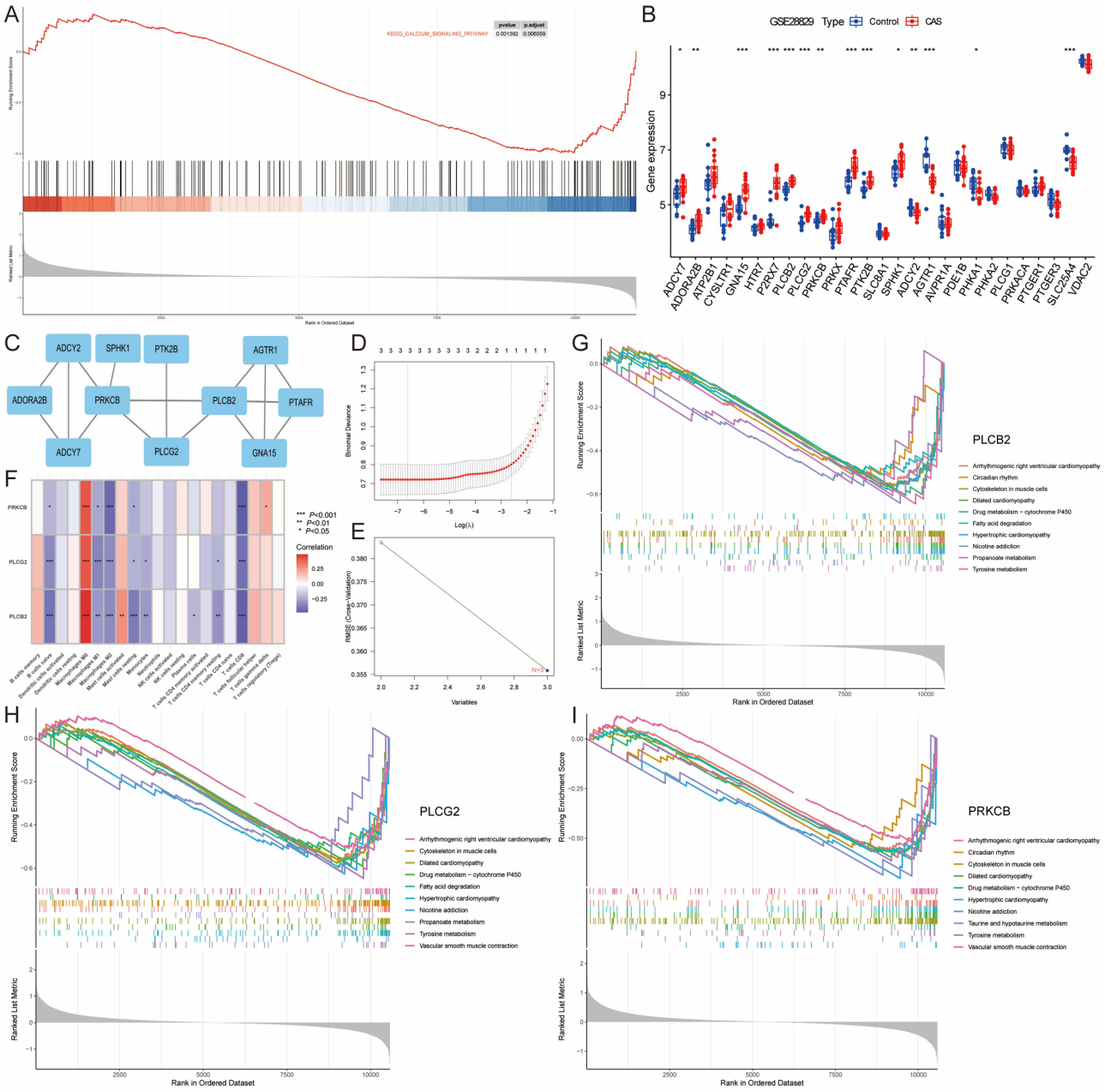

Figure 8 Identification and enrichment analysis of CaRGs. (**A**). GSEA analysis of the calcium signaling pathways. (**B**). CAS-related external dataset GSE28829 validates the expression of CaRGs. (**C**). PPI network of CARGs. (**D**). LASSO regression screening for characterized genes. (**E**). SVM-REF algorithm to screen the most suitable key genes. (**F**). Correlation analysis of the CaRGs with infiltrating immune cells. (**G-I**). Single-gene GESA for the PLCB2-high, PRKCB-high, and PLCG2-high subgroups. **P*<0.05, ***P*<0.01, ****P*<0.001.

Identification of Key Genes of the Calcium Signaling Pathway in CAS

To further delineate the key genes related to the calcium signaling pathway in OB and CAS, 14 DEGs were obtained by external validation using CAS-related dataset GSE28829, and a PPI network with 11 nodes and 16 edges was established (Figure 8B). Then, utilizing "CytoHubba" for topological analysis, three key genes (PLCB2, PRKCB, PLCG2) with degree centrality, betweenness centrality, and closeness centrality greater than the average were screened out, of which PRKCB was up-regulated in OB and CAS, while PLCB2 and PLCG2 were down-regulated (Figure 8C). LASSO regression and SVM-RFE similarly identified PLCB2, PRKCB, and PLCG2 as characteristic genes (Figure 8D and E). Consequently, these genes were identified as key genes in the calcium signaling pathway relevant to OB and CAS.

To elucidate the interplay between CaRGs and immune cells, immune cell correlation analysis showed that PLCB2, PRKCB, and PLCG2 were significantly negatively correlated with naïve B cells, M1 macrophages, M2 macrophages, resting mast cells, monocytes, and CD8 T cells, and significantly negatively correlated with M0 macrophages (Figure 8F). These correlations suggest that CaRGs may modulate the immune-infiltrating microenvironment in CAS, indicating a link between immune cell activation in CAS and the calcium signaling pathway.

In an effort to uncover the potential biological functions of CaRGs, single-gene GESA indicated that tyrosine metabolism, nicotine addiction, drug metabolism-cytochrome p450, hypertrophic cardiomyopathy, dilated cardiomyopathy, arrhythmogenic right ventricular cardiomyopathy, cytoskeleton in muscle cells, propanoate metabolism, circadian rhythm, and fatty acid degradation were significantly enriched in the PLCB2-high, PRKCB-high, and PLCG2-high subgroup (Figure 8G–I).

Validation of CaRGs and Construction of Nomogram

Subsequently, in vivo experiments showed that PLCB2 was significantly up-regulated in serum, adipose and aortic tissues of OB and AS model mice; PRKCB was down-regulated in aortic tissues and up-regulated in adipose tissues and serum; PLCG2 was up-regulated in aortic tissues of mice (Figure 9A). Therefore, PRKCB and PLCB2 were identified as key genes of the calcium signaling pathway in OB and CAS.

Additionally, in order to explore the diagnostic capability of calcium signaling pathway-related genes in OB and CAS, this study constructed a nomogram to predict the risk of developing OB and CAS based on PRKCB and PLCB2 (Figure 9B). The results of calibration and decision curves showed that the nomogram demonstrated satisfactory diagnostic efficacy (Figure 9C and D). Furthermore, the ROC curves showed that these genes exhibited satisfactory diagnostic performance in both the training and validation sets (AUC values greater than 0.80), suggesting that calcium signaling pathway-related genes may also serve be able to serve as potential biomarkers for OB and CAS (Figure 9E–H).

Discussion

OB and CAS are significant challenges to global public health. OB is not only a metabolic disorder but also associated with an increased risk of various cardiovascular diseases, including coronary heart disease, heart failure, and hypertension. These diseases are the leading causes of death and disability worldwide, imposing a significant economic burden on healthcare systems. According to the World Health Organization (WHO), more than 1.9 billion adults are overweight globally, with 650 million being obese, and this trend is increasing across different regions and age groups.[35] As a form of cardiovascular disease, CAS is a significant predictor of stroke and myocardial infarction, with its incidence rising alongside the increasing rates of OB.[36] Therefore, diagnosing or preventing cardiovascular diseases in the OB population is particularly important. The purpose of this study is to explore the potential mechanisms and biomarkers between OB and CAS. Although existing research has revealed the association between OB and CAS, the specific molecular mechanisms of these diseases are not yet fully understood. Identifying and validating key biomarkers in the process of these diseases is crucial for early diagnosis, risk stratification, and personalized treatment. Moreover, understanding the molecular links between OB and CAS may uncover new therapeutic targets, aiding in the development of more effective interventions.

In order to identify diagnostic biomarkers for CAS in OB population, this study obtained 3 CORGs (MMP9, PLA2G7, and SPP1) based on bioinformatics. MMP9, responsible for tissue remodeling and extracellular matrix protein degradation, are considered biomarkers of endothelial activation and dysfunction in cardiovascular disease, are strongly correlated with AS plaque instability and severity, and are also used as biomarkers of AS.[37,38] MMP9 is also highly expressed in obese children, adolescents, and adults, and MMP9 genotypes and haplotypes were found to influence MMP9 levels in obese children and adolescents.[39–43] In addition, MMP9 was positively correlated with body mass index ($r=0.40$, $P<0.01$) and negatively correlated with insulin sensitivity ($r=-0.46$, $P<0.001$).[40]

PLA2G7, also known as lipoprotein-associated phospholipase A2 (Lp-PLA2) and platelet-activating factor acetylhydrolase (PAF-AH), is a prominent enzyme within the phospholipase A2 superfamily. It is instrumental in the synthesis of ox-LDL, with its activity predominantly emanating from adipose tissue and adipocytes. PLA2G7 has garnered attention as a robust predictor of cardiovascular events, a role that has been corroborated by multiple studies observing its

https://doi.org/10.2147/JIR.S504480

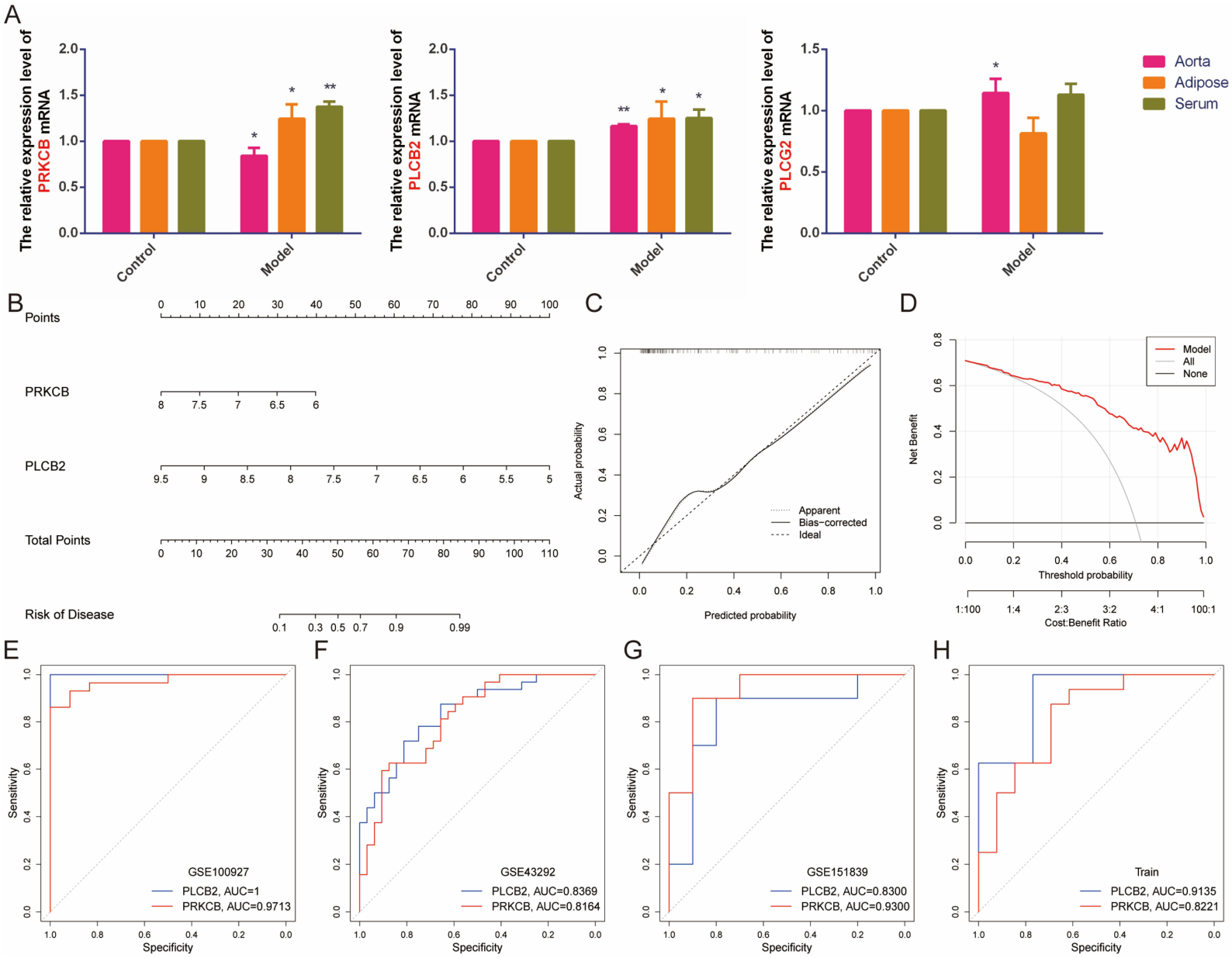

Figure 9 Construction of nomogram based on CaRGs to predict the risk of developing OB and CAS. (**A**). The relative expression level of PRKCB, PLCB2, and PLCG2 genes (*n*=6). **P*<0.05 vs the Control group, ***P*<0.01 vs the Control group. (**B**). Construction of a nomogram for predicting the risk of OB and CAS based on CaRGs. (**C** and **D**). Construction of a (**C**) calibration curve and (**D**) decision curve analysis for assessing the predictive efficiency of the nomogram model. (**E-H**). ROC curves were used for internal validation on CAS-related datasets (**E**) GSE100927 and (**F**) GSE43292 and OB-related dataset (**G**) GSE151839 and for external validation on CAS-related dataset (**H**) GSE28829.

heightened expression in CAS.[44–46] Furthermore, Lp-PLA2, which is derived from macrophages, has been identified as a catalyst for the destabilization of vulnerable atherosclerotic plaques, thus amplifying the risk of coronary events, and Lp-PLA2 inhibitors have been shown to reduce the frequency of these events.[45] In the context of OB, Lp-PLA2 is observed to be upregulated, with research indicating a positive correlation between its activity and Body Mass Index (BMI), and an inverse relationship with the adipokines leptin and lipocalin.[43,47,48] The impact of lifestyle interventions on PLA2G7 activity has also been noted, with exercise shown to decrease serum PAF-AH expression levels in obese women.[49,50] Thus, PLA2G7 has been recognized as a diagnostic biomarker of CAS and OB that predicts the development of OB and CAS.[46,48]

The elevated expression of SPP1 has been observed in patients with AS.[51] Studies indicate that SPP1-expressed osteopontin have adhesive, chemotactic, and calcium-binding properties, and that high expression in AS plaques may contribute to cellular accumulation and dystrophic calcification.[52] Overexpression of SPP1 notably promoted fatty streak formation, monocyte and lipid continuation, and inhibited IL-10 production by macrophages in high-fat diet mice.[53] Additionally, previous studies has identified SPP1 as a potential biomarker for the co-morbidities of AS and non-alcoholic fatty liver disease.[54]

Subsequently, Five Hub genes (CD52, CLEC5A, MMP9, FYB, and SPP1) were screened based on identified based on 61 machine learning models. CLEC5A, a C-type lectin receptor, is highly expressed in macrophages of atherosclerotic plaque lesions in advanced human and apoE$^{-/-}$ mice and is strongly associated with early AS plaque progression, promoting macrophage survival.[55] In obese populations, visceral and subcutaneous adipose tissue macrophage activation underlies OB metabolic disturbances. CLEC5A plays an important role in the transformation of adipose tissue macrophage subtypes and influences inflammatory responses during OB.[56]

CD52 is a glycosylphosphatidylinositol (GPI)-anchored glycoprotein, is widely expressed in immune cells. A bioinformatics analysis likewise identified CD52 as a potential diagnostic biomarker for AS, and high expression of the CD52 gene was observed in a foam cell model of ox-LDL-induced THP-1 cells.[57] Furthermore, elevated CD52 expression is also detected in unstable carotid atherosclerotic plaques, potentially linking its presence to cellular lipid accumulation and inflammatory processes.[58,59] Significant differential expression of CD52 was likewise identified in adipocytes and preadipocytes of obese and lean individuals, and CD52 was found to be a significantly upregulated mRNA in mature adipocytes and preadipocytes in both in vivo experiments in high-fat diet-fed mice and in vitro experiments in adipocytes.[60] Additionally, traditional Chinese medicine indicates that people with phlegm-dampness are more likely to suffer from OB and metabolic syndrome, and CD52 has a significantly high expression in phlegm-dampness.[61]

FYB, acting as an adaptor protein in the FYN and LCP2 signaling cascade within T cells, may play a role in linking T cell signaling to actin cytoskeleton remodeling.[62,63] FYB has been identified as a key gene in conditions such as OB combined with periodontitis and AS combined with psoriasis.[64,65] However, the specific mechanisms by which FYB regulates these conditions, particularly OB and AS, remain unclear.

In summary, this study identified MMP9, PLA2G7, CD52, CLEC5A, SPP1, and FYB as potential diagnostic biomarkers for CAS in the OB population through bioinformatics analysis and in vivo experiments. Other researchers have also investigated potential biomarkers for CAS. For instance, Huang identified autophagy-related genes CCL2, LAP2, and CTB associated with CAS using PPI network topology algorithms;[66] Wei recognized ANGPTL1, CX3CR1, and CCL4 as key genes for aortic valve calcification and CAS through LASSO regression;[67] Qin utilized various machine learning models, including LASSO regression, SVM, and RF, to identify C3AR1, FBLN5, PPP1R12A, and TPM1 as key genes for CAS.[68] The studies mentioned also concentrate on CAS; however, what distinguishes this particular study is its construction of multiple machine learning models. The models were carefully selected based on their F1 scores and accuracy, with a particular emphasis on assessing the risk of CAS within the OB population and examining the role of the calcium signaling pathway in comorbid conditions.

Additionally, studies have frequently highlighted the significance of the calcium signaling pathway in both OB and AS. Studies indicate that dietary calcium plays a crucial role in regulating energy metabolism and the risk of OB. Intracellular calcium ions are essential for the regulation of lipid metabolism and triglyceride storage in adipocytes. An increase in calcium ion levels can activate genes responsible for fat generation, promote lipid accumulation in adipocytes, and inhibit fat breakdown, leading to increased lipid deposition. A low-calcium diet can lead to elevated levels of

calcitriol, which in turn stimulates the influx of calcium ions into fat cells, fostering the development of OB.[69,70] Furthermore, the Ca^{2+}/calcium-sensing receptor (CaSR) is considered a potential mediator of white adipose tissue dysfunction. Research has shown that exposure of adipocytes to CaSR activators enhances the expression and secretion of pro-inflammatory cytokines. In a pro-inflammatory environment, white adipose tissue becomes dysfunctional, leading to increased fat deposition in peripheral organs and insulin resistance, thereby promoting the onset of OB.[71,72]

AS initiates with the migration of monocytes across the endothelial barrier, a process where an increase in intracellular free calcium concentration in endothelial cells significantly enhances monocyte adhesion.[73] Studies have shown that intracellular free regulates functions such as cell contraction, proliferation, migration and transcription, and that calcium transport proteins undergo biphasic changes as AS progresses.[74] The calcium signaling pathway is pivotal in modulating the susceptibility to AS and is deeply involved in the inflammatory processes that drive AS pathogenesis.[50,57] The calcium signaling pathway can regulate NF-κB inhibitor proteins through various molecular mechanisms, thereby affecting NF-κB activation, and this transcription factor can also participate in the activation of the calcium signaling pathway by regulating the expression and activity of various calcium channels.[75] The activation of the NF-κB pathway is involved in the regulation of cellular inflammation, proliferation, differentiation, and metabolism, all of which are indispensable parts of the AS pathogenesis.[76] Moreover, early evidence has shown the potential plaque-stabilizing effects of calcium channel blockers, which have been demonstrated to inhibit the thickening of the atherosclerotic intima and, to a certain extent, to ameliorate CAS.[77,78]

Mitochondrial calcium homeostasis is crucial for regulating cellular energy metabolism, respiration, cell death signaling, and redox balance. Dysfunction in mitochondria leads to calcium homeostasis imbalance and excessive reactive oxygen species production, which contribute to endothelial dysfunction, inflammatory cell recruitment, smooth muscle cell proliferation, and lipid deposition in the vascular wall, culminating in plaque formation and progression.[79]

The CaSR is instrumental in modulating intracellular calcium ion signaling and has been shown to alleviate endothelial inflammation in AS by regulating integrin β1 and NLRP3 inflammasomes.[80] Downregulation of CaSR expression promotes the progression of calcification in smooth muscle cells.[81] Inositol 1,4,5-trisphosphate receptors (IP3Rs) are essential for maintaining intracellular calcium ion homeostasis and are implicated in various programmed cell death pathways, including apoptosis, pyroptosis, and ferroptosis, thereby influencing cardiovascular diseases such as heart failure, ischemia, arrhythmias, and AS.[82]

Therefore, regulating mitochondrial calcium and ROS levels may offer novel therapeutic strategies for atherosclerosis. Targeting the calcium signaling pathway through interventions like calcium channel blockers and CaSR modulation could mitigate AS progression and provide new avenues for future therapeutic development.

This study also identified three CaCRs that are strongly associated with OB and AS, namely PLCB2, PRKCB, and PLCG2. In addition, enrichment analysis revealed that these genes play important roles in the phosphatidylinositol signaling system, neutrophil extracellular trap formation, and chemokine signaling pathway-related pathways. PLCB2 is instrumental in platelet activation, a process that is intricately linked to the pathogenesis of AS. The expression of the PLCB2 gene is modulated by NF-κB, which has been shown to implicate the development of AS by regulating inflammation and platelet activation through the NF-κB/ PLCB2 signaling axis.[83] Furthermore, PLCB2 is posited as a key gene associated with abnormal endothelial shear stress, Abnormal endothelial shear stress leads to activation of endothelial cells by the vascular endothelial system, which promotes the release of pro-inflammatory factors, leading to endothelial dysfunction and contributing to the progression of the subclinical stage of AS.[84] In addition, PLCB2 has been identified as a critical positive regulator of VEGF-induced vascular permeability by modulating calcium flux and phosphatidylinositol 4.5-bisphosphate levels at the cellular level.[85]

PLCG2 hydrolyzes membrane phospholipids into the second messenger molecules diacylglycerol and inositol 1,4,5-trisphosphate.[86] Studies have shown that PLCG2 is associated with inflammatory responses, NK cell immunity, and glycolipid metabolism and may interact with a high-fat diet to accelerate the progression of Alzheimer's disease in obese mice.[87–89] However, the relationship between PLCG2 and AS remains unclear.

PRKCB plays a multifaceted role in cellular processes, including the regulation of calcium signaling, apoptosis triggered by oxidative stress, and insulin resistance.[90] Research has demonstrated that PRKCB exerts a negative regulatory effect on the insulin-stimulated translocation of the glucose transporter protein SLC2A4/GLUT4, a key player

in glucose transport within adipocytes.[91] In endothelial cells, the overexpression of PRKCB isoforms has been linked to vascular insulin resistance and upregulation of endothelin-1, molecular changes that contribute to endothelial dysfunction and potentially exacerbate the progression of AS.[92] Furthermore, the activation of PRKCB in these cells leads to heightened phosphorylation of the retinoblastoma protein and increased cell proliferation in response to VEGFA. Concurrently, it disrupts the insulin-dependent activation of the PI3K/ AKT pathway, which in turn impairs the function of endothelial nitric oxide synthase (NOS3/eNOS), resulting in endothelial dysfunction.[93]

In conclusion, this study analysis highlighted the immune and inflammatory response, lipid metabolism, the calcium signaling pathway, and phagocytosis as potential mechanisms by which OB may promote AS. MMP9, PLA2G7, CD52, SPP1, FYB, PRKCB, CLEC57A, and PLCB2 genes were up-regulated in the serum of C57BL/6J ApoE$^{-/-}$ mice fed a high-fat diet. Therefore, MMP9, PLA2G7, CD52, CLEC5A, SPP1, and FYB were identified as potential biomarkers for the development of CAS in the obese population. PLCB2 and PRKCB are key genes in the calcium signaling pathway in OB and AS. These findings offer new insights into potential diagnostic biomarkers for CAS in obese populations and may guide future research directions to improve clinical management and treatment strategies for AS in obese patients, such as developing new treatment methods targeting specific pathways of these Hub genes. Furthermore, these findings underscore the importance of the calcium signaling pathway in the pathogenesis of OB and CAS, providing new targets for future research.

Although this study provides new insights into the potential links between OB and CAS and identifies several possible biomarkers, it also has some limitations. First, the datasets used in this study were sourced from specific public databases, which may introduce selection bias and affect the generalizability of the results. Second, while multiple machine learning models were employed to analyze the data, the predictive power of these models may be limited by the quality and quantity of the data. Additionally, the available OB-related datasets are insufficient in number, making it difficult to adequately represent the OB population. Furthermore, this study primarily focused on calcium signaling pathway-related genes, potentially overlooking other important molecular mechanisms. In the in vivo experiments, although biological validation was provided, the models used may not fully replicate the complexities of human OB and CAS. Finally, the findings need to be validated in larger and more diverse population cohorts to confirm the clinical applicability and effectiveness of these biomarkers. Future research should take these limitations into account and explore additional datasets and analytical methods to further validate and expand upon the current findings.

Conclusions

MMP9, PLA2G7, CD52, CLEC5A, SPP1, and FYB may serve as potential diagnostic biomarkers for CAS in obese populations. PLCB2 and PRKCB are key genes in the calcium signaling pathway in OB and CAS. These findings offer new insights into clinical management and therapeutic strategies for CAS in obese individuals.

Abbreviations

AS, Atherosclerosis; AUC, Area Under the Curve; CAS, Carotid Atherosclerosis; CaRGs, Calcium signaling pathway-related genes; CaSR, Calcium-sensing Receptor; CORGs, Carotid Atherosclerosis and Obesity Co-related Differentially Expressed Genes; DEGs, Differentially Expressed Genes; GBM, Gradient Boosting Machine; GEO, Gene Expression Omnibus; GSEA, Gene Set Enrichment Analysis; GSVA, Gene Set Variation Analysis; HE, Hematoxylin-Eosin; OB, Obesity; ORO, Oil Red O; RF, Random Forest; PPI, Protein-Protein Interaction; ROC, Receiver Operating Characteristic; SVM-RFE, Support Vector Machine-Recursive Feature Elimination; WGCNA, Weighted Gene Co-expression Network Analysis.

Data Sharing Statement

The following information was supplied regarding data availability: Data is available at NCBI GEO: GSE100927, GSE43292, GSE12828, GSE125771, GSE28829, and GSE151839.

Ethical Approval and Participation Consent

The dataset for this study was obtained from the publicly available GEO database. In accordance with Article 32, Items 1 and 2 of the "Ethical Review Regulations of Life Sciences and Medical Research Involving Humans", issued by the National Health Commission, Ministry of Education, Ministry of Science and Technology, and National Administration of Traditional Chinese Medicine in 2023, no additional ethical review is required for this study. All animal experiments were conducted under the supervision of the Ethics Committee of the Affiliated Hospital of Liaoning University of Traditional Chinese Medicine, with the ethical approval number 2023CS(DW)-028-01, and were in compliance with the GB/T 35892-2018 "Laboratory Animal-Guidelines for Ethical Review of Animal Welfare".

Funding

Liaoning Provincial Natural Science Foundation Joint Fund (No. 1700141103037); Liaoning Provincial Department of Education (No. 2024-JYTCB-069); The General Program of National Natural Science Foundation of China (82474479); Liaoning Provincial Department of Science and Technology (2024-MSLH-306); Liaoning University of Traditional Chinese Medicine Youth Innovation Team.

Disclosure

The authors report no conflicts of interest in this work.

References

1. Jastreboff AM, Kotz CM, Kahan S, Kelly AS, Heymsfield SB. Obesity as a disease: the obesity society 2018 position statement. *Obesity*. 2019;27(1):7–9. doi:10.1002/oby.22378
2. The National Health Commission's bureau of disease prevention and control. Report on the Nutrition and Chronic Disease Status of Chinese Residents. *Acta Nutrimenta Sinica*. 2020;42(6):521.
3. Bray GA, Heisel WE, Afshin A, et al. The science of obesity management: an endocrine society scientific statement. *Endocr Rev*. 2018;39(2):79–132. doi:10.1210/er.2017-00253
4. Libby P. The changing landscape of atherosclerosis. *Nature*. 2021;592(7855):524–533. doi:10.1038/s41586-021-03392-8
5. Marini S, Merino J, Montgomery BE, et al. Mendelian randomization study of obesity and cerebrovascular disease. *Ann Neurol*. 2020;87(4):516–524. doi:10.1002/ana.25686
6. Li M, Cui M, Li G, et al. The pathophysiological associations between obesity, NAFLD, and atherosclerotic cardiovascular diseases. *Horm Metab Res*. 2024;56(10):683–696. doi:10.1055/a-2266-1503
7. Lovren F, Teoh H, Verma S. Obesity and atherosclerosis: mechanistic insights. *Can J Cardiol*. 2015;31(2):177–183. doi:10.1016/j.cjca.2014.11.031
8. Song Z, Wang Y, Zhang F, Yao F, Sun C. Calcium signaling pathways: key pathways in the regulation of obesity. *Int J mol Sci*. 2019;20(11):2768. doi:10.3390/ijms20112768
9. Zemel MB, Shi H, Greer B, Dirienzo D, Zemel PC. Regulation of adiposity by dietary calcium. *FASEB j*. 2000;14(9):1132–1138. doi:10.1096/fasebj.14.9.1132
10. Davies KM, Heaney RP, Recker RR, et al. Calcium intake and body weight. *J Clin Endocrinol Metab*. 2000;85(12):4635–4638. doi:10.1210/jcem.85.12.7063
11. Tajbakhsh A, Kovanen PT, Rezaee M, Banach M, Sahebkar A. Ca(2+) flux: searching for a role in efferocytosis of apoptotic cells in atherosclerosis. *J Clin Med*. 2019;8(12):2047. doi:10.3390/jcm8122047
12. Kalampogias A, Siasos G, Oikonomou E, et al. Basic mechanisms in atherosclerosis: the role of calcium. *Med Chem*. 2016;12(2):103–113. doi:10.2174/1573406411666150928111446
13. Fan G, Cui Y, Gollasch M, Kassmann M. Elementary calcium signaling in arterial smooth muscle. *Channels*. 2019;13(1):505–519. doi:10.1080/19336950.2019.1688910
14. Yang Y, Xie E, Liu Y, et al. Calcium promotes vascular smooth muscle cell phenotypic switching in Marfan syndrome. *Biochem Biophys Res Commun*. 2023;665:124–132. doi:10.1016/j.bbrc.2023.05.017
15. Clough E, Barrett T. The gene expression omnibus database. *Methods mol Biol*. 2016;1418:93–110. doi:10.1007/978-1-4939-3578-9_5
16. Hägg DA, Olson FJ, Kjelldahl J, et al. Expression of chemokine (C-C motif) ligand 18 in human macrophages and atherosclerotic plaques. *Atherosclerosis*. 2009;204(2):e15–e20. doi:10.1016/j.atherosclerosis.2008.10.010
17. Karlöf E, Seime T, Dias N, et al. Correlation of computed tomography with carotid plaque transcriptomes associates calcification with lesion-stabilization. *Atherosclerosis*. 2019;288:175–185. doi:10.1016/j.atherosclerosis.2019.05.005
18. Ayari H, Bricca G. Identification of two genes potentially associated in iron-heme homeostasis in human carotid plaque using microarray analysis. *J Biosci*. 2013;38(2):311–315. doi:10.1007/s12038-013-9310-2
19. Steenman M, Espitia O, Maurel B, et al. Identification of genomic differences among peripheral arterial beds in atherosclerotic and healthy arteries. *Sci Rep*. 2018;8(1):3940. doi:10.1038/s41598-018-22292-y
20. Döring Y, Manthey HD, Drechsler M, et al. Auto-antigenic protein-DNA complexes stimulate plasmacytoid dendritic cells to promote atherosclerosis. *Circulation*. 2012;125(13):1673–1683. doi:10.1161/circulationaha.111.046755
21. Walker JM, Garcet S, Aleman JO, et al. Obesity and ethnicity alter gene expression in skin. *Sci Rep*. 2020;10(1):14079. doi:10.1038/s41598-020-70244-2

22. Gautier L, Cope L, Bolstad BM, Irizarry RA. affy–analysis of Affymetrix GeneChip data at the probe level. *Bioinformatics*. 2004;20(3):307–315. doi:10.1093/bioinformatics/btg405
23. Leek JT, Johnson WE, Parker HS, Jaffe AE, Storey JD. The sva package for removing batch effects and other unwanted variation in high-throughput experiments. *Bioinformatics*. 2012;28(6):882–883. doi:10.1093/bioinformatics/bts034
24. Ritchie ME, Phipson B, Wu D, et al. limma powers differential expression analyses for RNA-sequencing and microarray studies. *Nucleic Acids Res*. 2015;43(7):e47. doi:10.1093/nar/gkv007
25. Wilkerson MD, Hayes DN. ConsensusClusterPlus: a class discovery tool with confidence assessments and item tracking. *Bioinformatics*. 2010;26 (12):1572–1573. doi:10.1093/bioinformatics/btq170
26. Karuppagounder SS, Alin L, Chen Y, et al. N-acetylcysteine targets 5 lipoxygenase-derived, toxic lipids and can synergize with prostaglandin E(2) to inhibit ferroptosis and improve outcomes following hemorrhagic stroke in mice. *Ann Neurol*. 2018;84(6):854–872. doi:10.1002/ana.25356
27. Hu K. Become competent within one day in generating boxplots and violin plots for a novice without prior R experience. *Methods Protoc*. 2020;3 (4):64. doi:10.3390/mps3040064
28. Langfelder P, Horvath S. WGCNA: an R package for weighted correlation network analysis. *BMC Bioinf*. 2008;9:559. doi:10.1186/1471-2105-9-559
29. Kanehisa M, Furumichi M, Sato Y, Kawashima M, Ishiguro-Watanabe M. KEGG for taxonomy-based analysis of pathways and genomes. *Nucleic Acids Res*. 2023;51(D1):D587–D592. doi:10.1093/nar/gkac963
30. Zhou Y, Zhou B, Pache L, et al. Metascape provides a biologist-oriented resource for the analysis of systems-level datasets. *Nat Commun*. 2019;10 (1):1523. doi:10.1038/s41467-019-09234-6
31. Sherman BT, Hao M, Qiu J, et al. DAVID: a web server for functional enrichment analysis and functional annotation of gene lists (2021 update). *Nucleic Acids Res*. 2022;50(W1):W216–W221. doi:10.1093/nar/gkac194
32. Subramanian A, Tamayo P, Mootha VK, et al. Gene set enrichment analysis: a knowledge-based approach for interpreting genome-wide expression profiles. *Proc Natl Acad Sci U S A*. 2005;102(43):15545–15550. doi:10.1073/pnas.0506580102
33. Van Essen DC. Cortical cartography and caret software. *Neuroimage*. 2012;62(2):757–764. doi:10.1016/j.neuroimage.2011.10.077
34. Robin X, Turck N, Hainard A, et al. pROC: an open-source package for R and S+ to analyze and compare ROC curves. *BMC Bioinf*. 2011;12:77. doi:10.1186/1471-2105-12-77
35. Okunogbe A, Nugent R, Spencer G, Powis J, Ralston J, Wilding J. Economic impacts of overweight and obesity: current and future estimates for 161 countries. *BMJ Glob Health*. 2022;7(9):e009773. doi:10.1136/bmjgh-2022-009773
36. Mozaffarian D, Benjamin EJ, Go AS, et al. Heart disease and stroke statistics-2016 update: a report from the American heart association. *Circulation*. 2016;133(4):e38–360. doi:10.1161/cir.0000000000000350
37. Zhang J. Biomarkers of endothelial activation and dysfunction in cardiovascular diseases. *Rev Cardiovasc Med*. 2022;23(2):73. doi:10.31083/j.rcm2302073
38. Olejarz W, Łacheta D, Kubiak-Tomaszewska G. Matrix metalloproteinases as biomarkers of atherosclerotic plaque instability. *Int J mol Sci*. 2020;21(11):3946. doi:10.3390/ijms21113946
39. Luizon MR, Belo VA, Fernandes KS, Andrade VL, Tanus-Santos JE, Sandrim VC. Plasma matrix metalloproteinase-9 levels, MMP-9 gene haplotypes, and cardiovascular risk in obese subjects. *Mol Biol Rep*. 2016;43(6):463–471. doi:10.1007/s11033-016-3993-z
40. Unal R, Yao-Borengasser A, Varma V, et al. Matrix metalloproteinase-9 is increased in obese subjects and decreases in response to pioglitazone. *J Clin Endocrinol Metab*. 2010;95(6):2993–3001. doi:10.1210/jc.2009-2623
41. Belo VA, Souza-Costa DC, Luizon MR, et al. Matrix metalloproteinase-9 genetic variations affect MMP-9 levels in obese children. *Int J Obes Lond*. 2012;36(1):69–75. doi:10.1038/ijo.2011.169
42. Derosa G, Ferrari I, D'Angelo A, et al. Matrix metalloproteinase-2 and −9 levels in obese patients. *Endothelium*. 2008;15(4):219–224. doi:10.1080/10623320802228815
43. Nair S, Lee YH, Rousseau E, et al. Increased expression of inflammation-related genes in cultured preadipocytes/stromal vascular cells from obese compared with non-obese Pima Indians. *Diabetologia*. 2005;48(9):1784–1788. doi:10.1007/s00125-005-1868-2
44. Miwa Y, Kamide K, Takiuchi S, et al. Association of PLA2G7 polymorphisms with carotid atherosclerosis in hypertensive Japanese. *Hypertens Res*. 2009;32(12):1112–1118. doi:10.1038/hr.2009.151
45. Vickers KC, Maguire CT, Wolfert R, et al. Relationship of lipoprotein-associated phospholipase A2 and oxidized low density lipoprotein in carotid atherosclerosis. *J Lipid Res*. 2009;50(9):1735–1743. doi:10.1194/jlr.M800342-JLR200
46. Liu H, Yao Y, Wang Y, et al. Association between high-sensitivity C-reactive protein, lipoprotein-associated phospholipase A2 and carotid atherosclerosis: a cross-sectional study. *J Cell Mol Med*. 2018;22(10):5145–5150. doi:10.1111/jcmm.13803
47. Jackisch L, Kumsaiyai W, Moore JD, et al. Differential expression of Lp-PLA2 in obesity and type 2 diabetes and the influence of lipids. *Diabetologia*. 2018;61(5):1155–1166. doi:10.1007/s00125-018-4558-6
48. Seyfarth J, Reinehr T, Hoyer A, et al. Lipoprotein-associated phospholipase A2 activity in obese adolescents with and without type 2 diabetes. *J Inherit Metab Dis*. 2018;41(1):73–79. doi:10.1007/s10545-017-0100-0
49. Woudberg NJ, Mendham AE, Katz AA, Goedecke JH, Lecour S. Exercise intervention alters HDL subclass distribution and function in obese women. *Lipids Health Dis*. 2018;17(1):232. doi:10.1186/s12944-018-0879-1
50. Wootton PT, Flavell DM, Montgomery HE, World M, Humphries SE, Talmud PJ. Lipoprotein-associated phospholipase A2 A379V variant is associated with body composition changes in response to exercise training. *Nutr Metab Cardiovasc Dis*. 2007;17(1):24–31. doi:10.1016/j.numecd.2005.11.008
51. Wolak T. Osteopontin - a multi-modal marker and mediator in atherosclerotic vascular disease. *Atherosclerosis*. 2014;236(2):327–337. doi:10.1016/j.atherosclerosis.2014.07.004
52. O'Brien ER, Garvin MR, Stewart DK, et al. Osteopontin is synthesized by macrophage, smooth muscle, and endothelial cells in primary and restenotic human coronary atherosclerotic plaques. *Arterioscler Thromb*. 1994;14(10):1648–1656. doi:10.1161/01.atv.14.10.1648
53. Isoda K, Kamezawa Y, Ayaori M, Kusuhara M, Tada N, Ohsuzu F. Osteopontin transgenic mice fed a high-cholesterol diet develop early fatty-streak lesions. *Circulation*. 2003;107(5):679–681. doi:10.1161/01.cir.0000055739.13639.d7
54. Wu X, Yuan C, Pan J, et al. CXCL9, IL2RB, and SPP1, potential diagnostic biomarkers in the co-morbidity pattern of atherosclerosis and non-alcoholic steatohepatitis. *Sci Rep*. 2024;14(1):16364. doi:10.1038/s41598-024-66287-4

55. Xiong W, Wang H, Lu L, et al. The macrophage C-type lectin receptor CLEC5A (MDL-1) expression is associated with early plaque progression and promotes macrophage survival. *J Transl Med*. 2017;15(1):234. doi:10.1186/s12967-017-1336-z
56. Girón-Ulloa A, González-Domínguez E, Klimek RS, et al. Specific macrophage subsets accumulate in human subcutaneous and omental fat depots during obesity. *Immunol Cell Biol*. 2020;98(10):868–882. doi:10.1111/imcb.12380
57. Zheng Z, Yuan D, Shen C, Zhang Z, Ye J, Zhu L. Identification of potential diagnostic biomarkers of atherosclerosis based on bioinformatics strategy. *BMC Med Genomics*. 2023;16(1):100. doi:10.1186/s12920-023-01531-w
58. Jiang J, Hiron TK, Agbaedeng TA, et al. A novel macrophage subpopulation conveys increased genetic risk of coronary artery disease. *Circ Res*. 2024;135(1):6–25. doi:10.1161/circresaha.123.324172
59. Agardh HE, Folkersen L, Ekstrand J, et al. Expression of fatty acid-binding protein 4/aP2 is correlated with plaque instability in carotid atherosclerosis. *J Intern Med*. 2011;269(2):200–210. doi:10.1111/j.1365-2796.2010.02304.x
60. Mao R, Yang F, Zhang Y, et al. High expression of CD52 in adipocytes: a potential therapeutic target for obesity with type 2 diabetes. *Aging*. 2021;13(8):11043–11060. doi:10.18632/aging.202714
61. Wang J, Wang Q, Li L, et al. Phlegm-dampness constitution: genomics, susceptibility, adjustment and treatment with traditional Chinese medicine. *Am J Chin Med*. 2013;41(2):253–262. doi:10.1142/s0192415x13500183
62. Kliche S, Breitling D, Togni M, et al. The ADAP/SKAP55 signaling module regulates T-cell receptor-mediated integrin activation through plasma membrane targeting of Rap1. *mol Cell Biol*. 2006;26(19):7130–7144. doi:10.1128/mcb.00331-06
63. Krause M, Sechi AS, Konradt M, Monner D, Gertler FB, Wehland J. Fyn-binding protein (Fyb)/SLP-76-associated protein (SLAP), Ena/vasodilator-stimulated phosphoprotein (VASP) proteins and the Arp2/3 complex link T cell receptor (TCR) signaling to the actin cytoskeleton. *J Cell Biol*. 2000;149(1):181–194. doi:10.1083/jcb.149.1.181
64. Su W, Zhao Y, Wei Y, Zhang X, Ji J, Yang S. Exploring the pathogenesis of psoriasis complicated with atherosclerosis via microarray data analysis. *Front Immunol*. 2021;12:667690. doi:10.3389/fimmu.2021.667690
65. Cai Y, Zuo X, Zuo Y, et al. Transcriptomic analysis reveals shared gene signatures and molecular mechanisms between obesity and periodontitis. *Front Immunol*. 2023;14:1101854. doi:10.3389/fimmu.2023.1101854
66. Huang T, Su C, Su Q, et al. Identification and validation of three diagnostic autophagy-related genes associated with advanced plaques and immune cell infiltration in carotid atherosclerosis based on integrated bioinformatics analyses. *PeerJ*. 2024;12:e18543. doi:10.7717/peerj.18543.
67. Wei K, Cao Y, Kong X, Liu C, Gu X. Exploration and validation of immune and therapeutic-related hub genes in aortic valve calcification and carotid atherosclerosis. *J Inflamm Res*. 2024;17:6485–6500. doi:10.2147/jir.S462546
68. Qin X, Ding R, Lu H, et al. Identification of pivotal genes and regulatory networks associated with atherosclerotic carotid artery stenosis based on comprehensive bioinformatics analysis and machine learning. *Front Pharmacol*. 2024;15:1364160. doi:10.3389/fphar.2024.1364160
69. Zemel MB. Regulation of adiposity and obesity risk by dietary calcium: mechanisms and implications. *J Am Coll Nutr*. 2002;21(2):146s–151s. doi:10.1080/07315724.2002.10719212
70. Zemel MB, Miller SL. Dietary calcium and dairy modulation of adiposity and obesity risk. *Nutr Rev*. 2004;62(4):125–131. doi:10.1111/j.1753-4887.2004.tb00034.x
71. Bravo-Sagua R, Mattar P, Díaz X, Lavandero S, Cifuentes M. Calcium sensing receptor as a novel mediator of adipose tissue dysfunction: mechanisms and potential clinical implications. *Front Physiol*. 2016;7:395. doi:10.3389/fphys.2016.00395
72. Rocha G, Villalobos E, Fuentes C, et al. Preadipocyte proliferation is elevated by calcium sensing receptor activation. *mol Cell Endocrinol*. 2015;412:251–256. doi:10.1016/j.mce.2015.05.011
73. Himi N, Hamaguchi A, Hashimoto K, Koga T, Narita K, Miyamoto O. Calcium influx through the TRPV1 channel of endothelial cells (ECs) correlates with a stronger adhesion between monocytes and ECs. *Adv Med Sci*. 2012;57(2):224–229. doi:10.2478/v10039-012-0044-4
74. Badin J, Rodenbeck S, McKenney-Drake ML, Sturek M. Multiphasic changes in smooth muscle Ca(2+) transporters during the progression of coronary atherosclerosis. *Curr Top Membr*. 2022;90:95–121. doi:10.1016/bs.ctm.2022.09.007
75. Bresnick AR, Weber DJ, Zimmer DB. S100 proteins in cancer. *Nat Rev Cancer*. 2015;15(2):96–109. doi:10.1038/nrc3893
76. Li W, Jin K, Luo J, et al. NF-κB and its crosstalk with endoplasmic reticulum stress in atherosclerosis. *Front Cardiovasc Med*. 2022;9:988266. doi:10.3389/fcvm.2022.988266
77. Ustünes L, Yasa M, Kerry Z, et al. Effect of verapamil on intimal thickening and vascular reactivity in the collared carotid artery of the rabbit. *Br J Pharmacol*. 1996;118(7):1681–1688. doi:10.1111/j.1476-5381.1996.tb15592.x
78. Mason RP. Mechanisms of plaque stabilization for the dihydropyridine calcium channel blocker amlodipine: review of the evidence. *Atherosclerosis*. 2002;165(2):191–199. doi:10.1016/s0021-9150(01)00729-8
79. Priya HK, Jha KP, Kumar N, Singh S. Reactive oxygen species and mitochondrial calcium's roles in the development of atherosclerosis. *Curr Pharm Des*. 2024;30(23):1812–1821. doi:10.2174/0113816128303026240514111200
80. Jiang Y, Xing W, Li Z, et al. The calcium-sensing receptor alleviates endothelial inflammation in atherosclerosis through regulation of integrin β1-NLRP3 inflammasome. *FEBS J*. 2024;292:191–205. doi:10.1111/febs.17308
81. Peterlik M, Kállay E, Cross HS. Calcium nutrition and extracellular calcium sensing: relevance for the pathogenesis of osteoporosis, cancer and cardiovascular diseases. *Nutrients*. 2013;5(1):302–327. doi:10.3390/nu5010302
82. Piamsiri C, Fefelova N, Pamarthi SH, et al. Potential roles of IP(3) receptors and calcium in programmed cell death and implications in cardiovascular diseases. *Biomolecules*. 2024;14(10):1334. doi:10.3390/biom14101334
83. Mao G, Jin J, Kunapuli SP, Rao AK. Nuclear factor-κB regulates expression of platelet phospholipase C-β2 (PLCB2). *Thromb Haemost*. 2016;116(5):931–940. doi:10.1160/th15-09-0749
84. Zhu G, Lai Y, Chen F, et al. Exploration of the crucial genes and molecular mechanisms mediating atherosclerosis and abnormal endothelial shear stress. *Dis Markers*. 2022;2022:6306845. doi:10.1155/2022/6306845
85. Phoenix KN, Yue Z, Yue L, et al. PLCβ2 promotes VEGF-induced vascular permeability. *Arterioscler Thromb Vasc Biol*. 2022;42(10):1229–1241. doi:10.1161/atvbaha.122.317645
86. Zhou Q, Lee GS, Brady J, et al. A hypermorphic missense mutation in PLCG2, encoding phospholipase Cγ2, causes a dominantly inherited autoinflammatory disease with immunodeficiency. *Am J Hum Genet*. 2012;91(4):713–720. doi:10.1016/j.ajhg.2012.08.006
87. Alinger JB, Mace EM, Porter JR, et al. Human PLCG2 haploinsufficiency results in a novel natural killer cell immunodeficiency. *J Allergy Clin Immunol*. 2024;153(1):216–229. doi:10.1016/j.jaci.2023.09.002

88. Tsai AP, Dong C, Lin PB, et al. PLCG2 is associated with the inflammatory response and is induced by amyloid plaques in Alzheimer's disease. *Genome Med*. 2022;14(1):17. doi:10.1186/s13073-022-01022-0
89. Oblak AL, Kotredes KP, Pandey RS, et al. Plcg2(M28L) interacts with high fat/high sugar diet to accelerate alzheimer's disease-relevant phenotypes in mice. *Front Aging Neurosci*. 2022;14:886575. doi:10.3389/fnagi.2022.886575
90. Kang SW, Wahl MI, Chu J, et al. PKCbeta modulates antigen receptor signaling via regulation of Btk membrane localization. *EMBO j*. 2001;20 (20):5692–5702. doi:10.1093/emboj/20.20.5692
91. Lee EE, Ma J, Sacharidou A, et al. A protein kinase C phosphorylation motif in GLUT1 affects glucose transport and is mutated in GLUT1 deficiency syndrome. *Mol Cell*. 2015;58(5):845–853. doi:10.1016/j.molcel.2015.04.015
92. Li Q, Park K, Li C, et al. Induction of vascular insulin resistance and endothelin-1 expression and acceleration of atherosclerosis by the overexpression of protein kinase C-β isoform in the endothelium. *Circ Res*. 2013;113(4):418–427. doi:10.1161/circresaha.113.301074
93. Yamasaki T, Takahashi A, Pan J, Yamaguchi N, Yokoyama KK. Phosphorylation of activation transcription factor-2 at serine 121 by protein kinase C controls c-Jun-mediated activation of transcription. *J Biol Chem*. 2009;284(13):8567–8581. doi:10.1074/jbc.M808719200